possibility, insulin-induced glucose uptake was measured in the cells with various concentrations of glucose. Fig. 2*E* shows that the GH-induced inhibition of glucose uptake was independent of glucose concentration, suggesting that glucose metabolism was not inhibited by GH pretreatment. Taken together, these data indicate that chronic GH pretreatment did not affect insulin-stimulated GLUT4 translocation or exofacial exposure (fusion) with the plasma membrane but that the reduction in glucose uptake primarily reflects changes in glucose transport activity.

Chronic GH Pretreatment Inhibits Insulin-dependent Activation of PI 3-Kinase Bound to IRS-2 and Akt Phosphorylation—GH binding to the GH receptor activates the JAK tyrosine kinase pathway that can also signal through IRS tyrosine phosphorylation. To investigate the effect of chronic GH pretreatment on insulin signaling pathways, fully differentiated 3T3-L1 adipocytes were pretreated with 100 nM GH for 24 h followed by stimulation with 0.1 nM insulin, and the activation of signal target molecules in response to insulin stimulation was assessed. We confirmed that GH pretreatment induced JAK2 tyrosine phosphorylation, and insulin receptor tyrosine phosphorylation, which is known to reflect tyrosine kinase activation, was not changed by GH pretreatment (Fig. 3*A*). Insulin-induced IRS-1 and IRS-2 tyrosine phosphorylation was slightly enhanced by GH pretreatment (Fig. 3*B*). However, GH stimulation itself increased both IRS-1 and IRS-2 tyrosine phosphorylation. The amount of the p85 PI 3-kinase regulatory subunit associated with IRS-1 and IRS-2 was also enhanced by GH treatment, which reflected enhancement of IRS tyrosine phosphorylation (Fig. 3*B*). IRS-1-associated PI 3-kinase activity was also enhanced by GH pretreatment (Fig. 3*C*, *left panel*). Surprisingly, IRS-2-associated PI 3-kinase activity was suppressed by GH treatment even though the amount of PI 3-kinase associated with IRS-2 was enhanced (Fig. 3*C*, *right panel*).

IRS-dependent activation of the PI 3-kinase generates the production of PIP_3 that is necessary for the phosphorylation of Akt on Ser-473 and Thr-308, resulting in the activation of Akt kinase activity. As shown in Fig. 3*D*, Akt phosphorylation was also inhibited by chronic GH pretreatment and that inhibition correlated with the suppression of IRS-2-associated PI 3-kinase activity.

IRS-2 Mediates the GH Inhibition of Insulin-stimulated Glucose Uptake—Data presented in Fig. 3 suggest that IRS-2 coupling to Akt activation may be the target of GH that is responsible for the inhibition of insulin-stimulated glucose uptake. As observed previously, GH pretreatment suppressed insulin-stimulated Akt phosphorylation in LacZ adenovirus-infected cells (Fig. 4*A*, *left panel*). In contrast, overexpression of IRS-2 by adenovirus infection completely protected against the inhibition of insulin-stimulated Akt phosphorylation by GH pretreatment (Fig. 4*A*, *right panel*). The restoration of insulin-stimulated Akt phosphorylation by IRS-2 overexpression occurred concomitant with the recovery of insulin-stimulated glucose uptake in the GH-pretreated cells (Fig. 4*B*). In parallel, expression of a constitutively active Akt mutant (myr-Akt) resulted in the basal increase in glucose uptake that was no longer insulin-sensitive (Fig. 4*C*). Importantly, myr-Akt expression completely protected the cells from the GH inhibition of insulin-stimulated glucose uptake.

If IRS-2-dependent regulation of Akt activation is the site of GH-induced insulin resistance, then reduction of IRS-2 levels should mimic the effect of GH pretreatment. To test this hypothesis, we reduced IRS-1 or IRS-2 protein levels by RNA interference-mediated gene silencing (Fig. 5). 3T3-L1 adipocytes were electroporated with an IRS-1- or IRS-2-specific siRNA that resulted in a marked reduction in targeted IRS protein levels without any significant effect on the other IRS protein level (Fig. 5*A*). IRS-1 knockdown had no significant effect on insulin-stimulated Akt activation, GLUT4 translocation, or glucose uptake (Fig. 5, *A–C*). On the other hand, in IRS-2 knockdown cells, there was a reduction in insulin-stimulated Akt phosphorylation (Fig. 5*A*). Although GLUT4 translocation to plasma membrane in response to insulin was not inhibited by IRS-2 knockdown (Fig. 5*B*), insulin-induced glucose uptake was significantly inhibited by the reduction in IRS-2 protein levels similar to that observed for chronic GH pretreatment (Fig. 5*C*).

DISCUSSION

In this study, we have observed that chronic GH pretreatment does not impair insulin-stimulated GLUT4 translocation to plasma membrane, yet results in a reduction in insulin-stimulated glucose uptake. Recently, several studies have also observed an apparent uncoupling of GLUT4 translocation and glucose uptake. For example, in L6 rat skeletal muscle cells, high leptin levels reduced insulin-stimulated glucose uptake despite normal GLUT4 translocation (36). Nelson *et al.* (37) suggested that, in 3T3-L1 adipocytes, high glucose levels impaired GLUT4 intrinsic activity. Smith *et al.* (38) reported that genistein, an inhibitor of tyrosine kinase, inhibited insulin-stimulated glucose transport without affecting translocation of GLUT4 in isolated rat adipocytes. PBP10, a rhodamine B-labeled 10-amino-acid peptide, which binds to phosphoinositides, itself induced GLUT4 translocation to the plasma membrane, without any increase in glucose uptake (39). Taken together with these reports, our data indicate that GLUT4 translocation and fusion with the plasma membrane are not sufficient to enhance glucose uptake *per se* but that additional activation steps are required. Thus, by comparing glucose uptake with GLUT4 translocation, we have successfully separated GLUT4-mediated glucose uptake into GLUT4 translocation step and activation step.

Previously, we have reported that adipose and muscle tissue isolated from human GH transgenic rat display insulin resistance and proposed that this resulted from an impairment of GLUT4 activation *in vivo* (23). To examine the potential mechanism(s), we determined the effect of GH pretreatment in cultured 3T3-L1 adipocytes. The current data demonstrate that chronic GH pretreatment impaired insulin-induced activation of PI 3-kinase bound to IRS-2, but not to IRS-1, leading to inhibition of insulin-induced glucose uptake without affecting GLUT4 translocation. IRS-2 overexpression or myr-Akt expression restored GH-induced

Downloaded from www.jbc.org at HIROSHIMA UNIVERSITY, on February 20, 2010

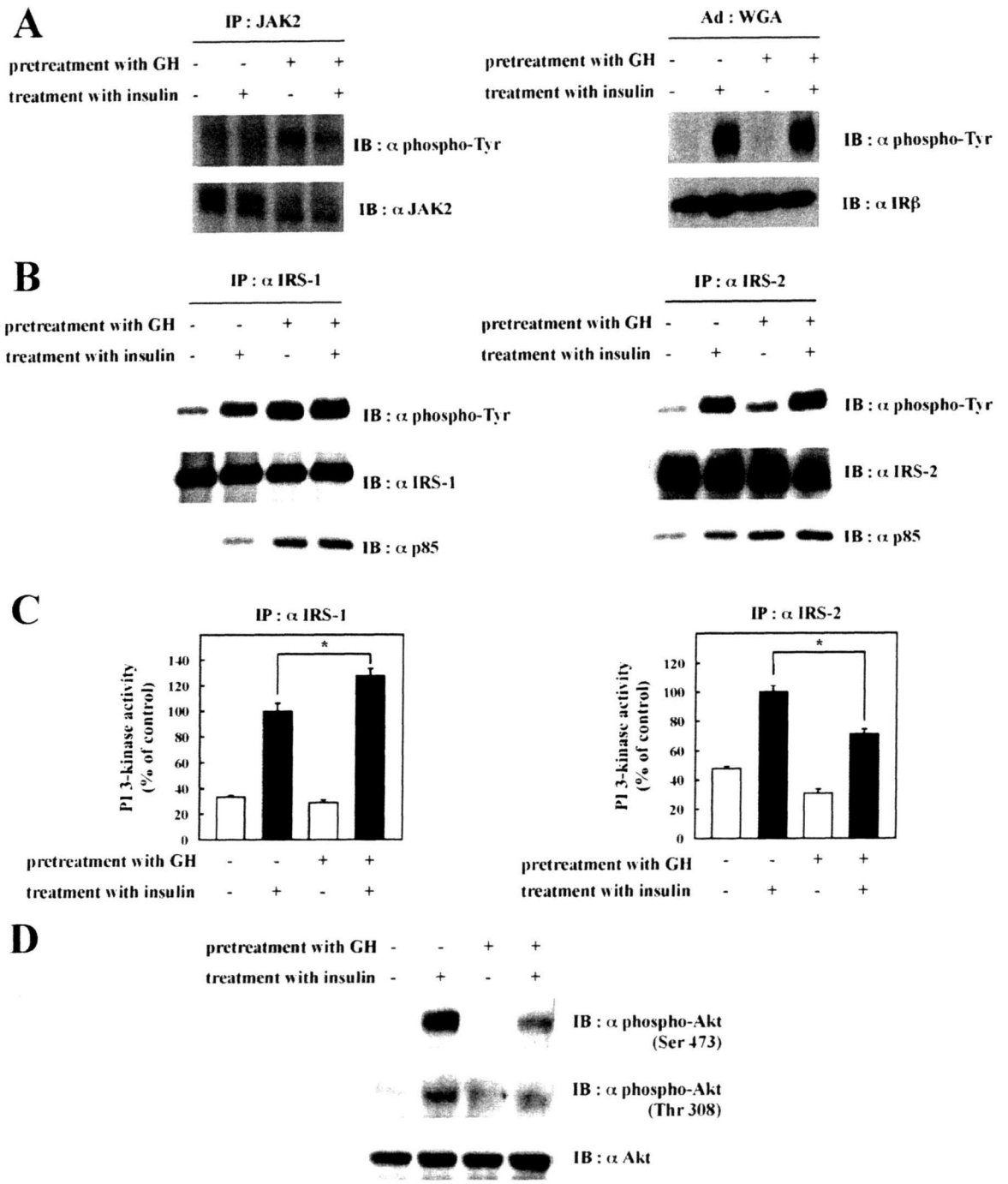

FIGURE 3. **Effects of chronic GH pretreatment on insulin signal activation.** After being serum-starved for 2 h, 3T3-L1 adipocytes were pretreated with or without 100 nM GH for 24 h and then treated with or without 0.1 nM insulin for 5 min. Cells were solubilized with Tris/Triton lysis buffer. *A*, whole cell lysates were immunoprecipitated (*IP*) with anti-JAK2 antibody, and the immunoprecipitates were subjected to immunoblotting (*IB*) with anti-phosphotyrosine or anti-JAK2 antibody (*left panel*). Insulin receptor was semi-purified with wheat germ agglutinin (*WGA*)-agarose from whole cell lysates. Semi-purified insulin receptor was separated by SDS-PAGE and immunoblotted with anti-phosphotyrosine antibody or anti-insulin receptor-β antibody (*right panel*). *B*, whole cell lysates were immunoprecipitated with anti-IRS-1 antibody or anti-IRS-2 antibody. Immunoprecipitates were separated by SDS-PAGE and immunoblotted with anti-phosphotyrosine antibody, anti-IRS-1 antibody, anti-IRS-2 antibody, or anti-p85 PI 3-kinase antibody. *C*, whole cell lysates were immunoprecipitated with anti-IRS-1 antibody or anti-IRS-2 antibody. PI 3-kinase activity in the immunocomplexes was measured as described under "Experimental Procedures." PI 3-kinase activities were quantified, and the results are presented as the means ± S.E. of three independent experiments. The difference between insulin-stimulated cells with and without GH pretreatment is significant with $p < 0.05$ (*). *D*, whole cell lysates were separated by SDS-PAGE and immunoblotted with anti-phospho-Akt (Ser-473) antibody, anti-phospho-Akt (Thr-308) antibody, or anti-Akt antibody.

impairment of insulin-dependent glucose uptake. In addition, IRS-2 knockdown showed similar phenotype to chronic GH pretreatment. These data revealed that chronic GH pretreatment reduced IRS-2-PI 3-kinase-Akt pathway, and this reduction was the reason why glucose uptake was impaired in GH-pretreated cells. Consistent with this interpretation,

Downloaded from www.jbc.org at HIROSHIMA UNIVERSITY, on February 20, 2010

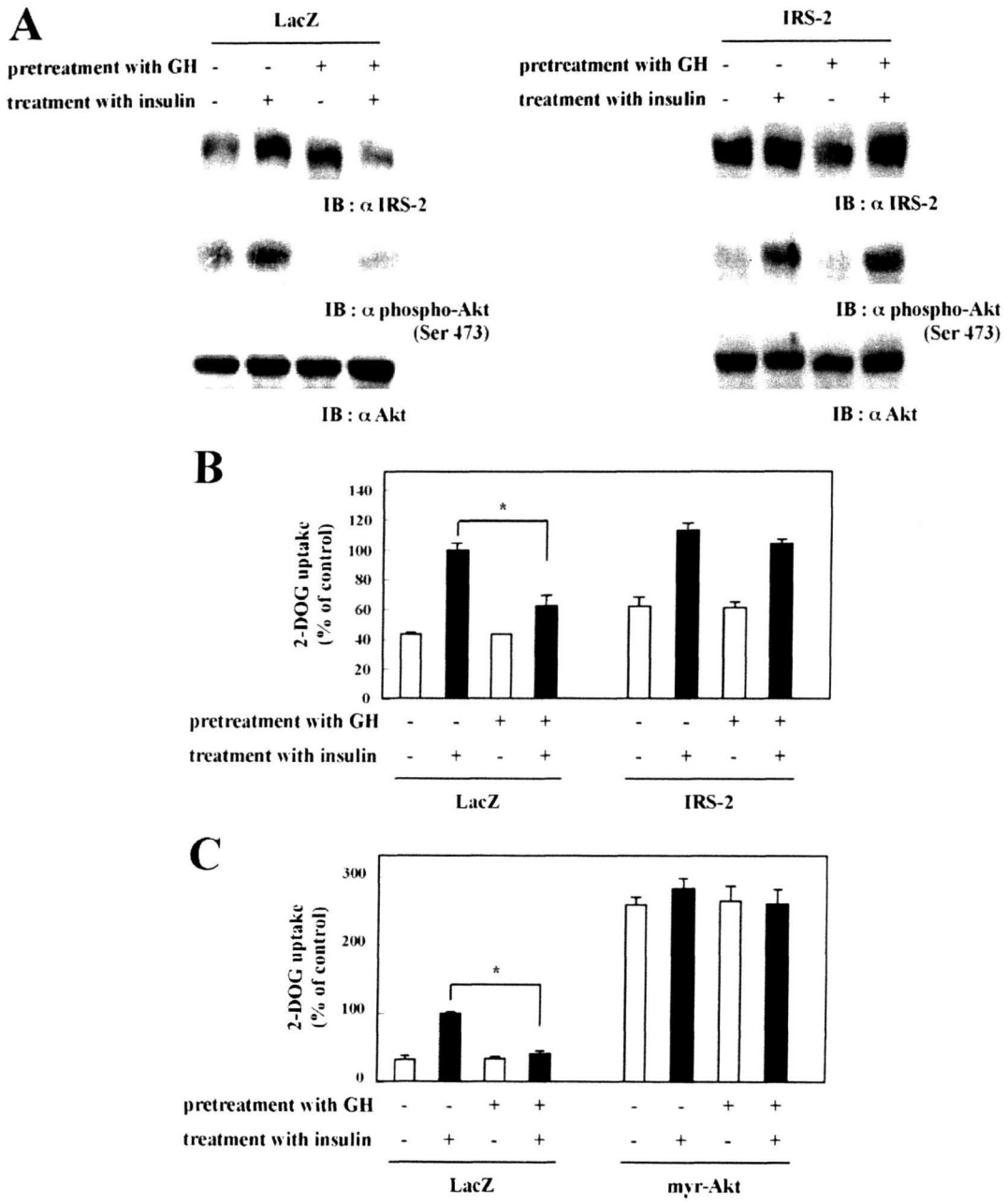

FIGURE 4. **Effects of IRS-2 or myr-Akt overexpression on glucose uptake.** 3T3-L1 adipocytes were infected with adenovirus containing cDNA encoding LacZ or IRS-2. Forty eight hours after infection, cells were serum-starved for 2 h and then pretreated with or without 100 nM GH for 24 h, followed by stimulation with or without 0.1 nM insulin for 20 min. *A*, cells were solubilized with Tris/Triton lysis buffer. Whole cell lysates were separated by SDS-PAGE and immunoblotted (*IB*) with anti-phospho-Akt (Ser-478) antibody and anti-Akt antibody. *B*, cells were assayed for glucose uptake as described under "Experimental Procedures." The results are presented as the means ± S.E. of five wells. The difference between insulin-stimulated cells with and without GH pretreatment is significant with $p < 0.01$ (*). *C*, 3T3-L1 adipocytes were infected with adenovirus containing cDNA encoding LacZ or myristoylated Akt (*myr-Akt*). Forty eight hours after infection, cells were serum-starved for 2 h, then pretreated with or without 100 nM GH for 24 h followed by stimulation with or without 0.1 nM insulin for 20 min, and assayed for glucose uptake as described under "Experimental Procedures." The results are presented as the means ± S.E. of five wells. The difference between insulin-stimulated cells with and without GH pretreatment is significant with $p < 0.01$ (*).

IRS-1 knockdown did not affect insulin-induced glucose uptake, suggesting that it is possible that PI 3-kinase associated with IRS-1 or IRS-2 facilitates different roles in glucose uptake. Similarly, studies using siRNA-mediated gene silencing revealed different functions for IRS-1 and IRS-2 in L6 myotube cells (40). We have reported that IRS-1 and IRS-2 showed different localization in COS-7 cells (41), suggesting that IRS-1 and IRS-2 are not functionally identical and therefore could result in differential spatial localization of PI 3-kinase.

Analyses of insulin signal activation revealed that chronic GH treatment impaired IRS-2-associated PI 3-kinase activity even though the amount of PI 3-kinase p85 regulatory subunit bound to IRS-2 was enhanced. There are several alternative

Downloaded from www.jbc.org at HIROSHIMA UNIVERSITY, on February 20, 2010

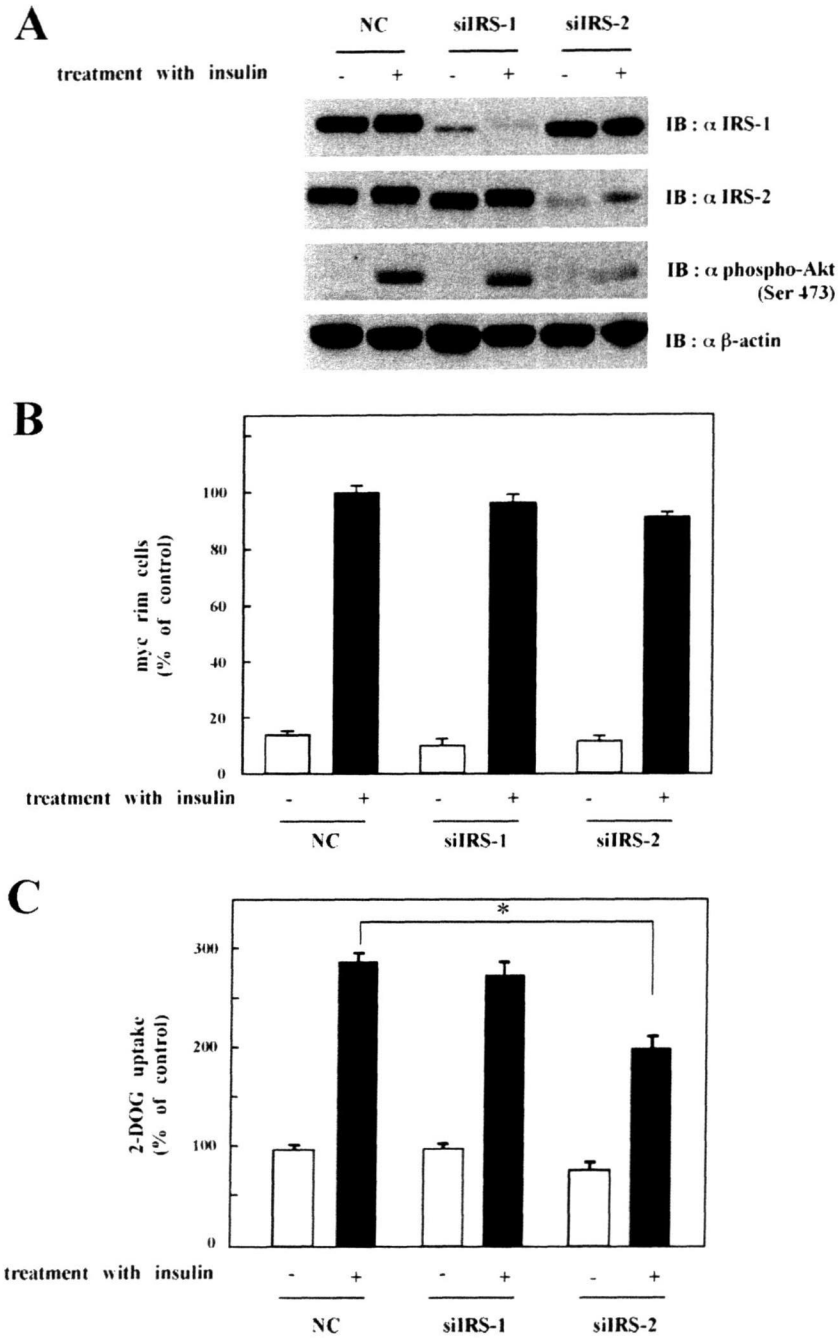

FIGURE 5. **Effects of IRS-2 knockdown on Akt activation and glucose uptake.** *A*, 3T3-L1 adipocytes were electroporated with siRNA against nonrelevant control (*NC*), against IRS-1 (*siIRS-1*), or against IRS-2 (*siIRS-2*) as described under "Experimental Procedures." Twenty four hours after electroporation, cells were serum-starved for 24 h. After washing, cells were treated with or without 100 nM insulin for 20 min. Cells were solubilized with Tris/Triton lysis buffer. Whole cell lysates were separated by SDS-PAGE and immunoblotted (*IB*) with anti-IRS-1 antibody, anti-IRS-2 antibody, anti-phospho-Akt (Ser-473), or anti-β-actin antibody. *B*, 3T3-L1 adipocytes were electroporated with siRNA against nonrelevant control (*NC*), against IRS-1 (*siIRS-1*), or against IRS-2 (*siIRS-2*) along with pGLUT4-myc-GFP. Twenty four hours after electroporation, cells were serum-starved for 2 h and then treated with or without 100 nM insulin for 20 min. Cells were then fixed without permeabilization and immunostained with anti-Myc antibody to detect cells with GLUT4 fused to plasma membrane. Average of percentage of cells showing GLUT4-myc-GFP rim on the cell surface was calculated. The ratio of GLUT4-myc on the cell surface in insulin-stimulated nonrelevant control cells was used as control. *C*, 3T3-L1 adipocytes were electroporated with siRNA against nonrelevant control (*NC*), against IRS-1 (*siIRS-1*), or against IRS-2 (*siIRS-2*). Cells were assayed for glucose uptake as described under "Experimental Procedures." The results are presented as the means ± S.E. of five wells. Glucose uptake by the nonrelevant control cells without insulin was used as control. The difference between insulin-stimulated cells electroporated with siRNA against nonrelevant control and IRS-2 is significant with $p < 0.001$ (*).

hypotheses that might account for the suppression of IRS-2-associated PI 3-kinase activity despite a physical increase in the amount of PI 3-kinase binding. First, some proteins, which bind to IRS-2, but not to IRS-1, in a GH-dependent manner, inhibited PI 3-kinase activation. It is well known that several proteins, including PTEN, that have phosphatidylinositol phosphatase activity antagonize the PI 3-kinase activity. These proteins could be candidates for GH-induced IRS-2-associated protein. Alternatively, chronic GH treatment induced post-translational modification of IRS-2 and not IRS-1 leading to the inability of IRS-2 to activate PI 3-kinase. Recently, we reported that IRS-associated protein, 53BP2S, impaired GLUT4 translocation to the plasma membrane (26). Thus proteins that bind to IRS might modulate the insulin signals through inhibition of IRS-2-associated PI 3-kinase activity.

Surprisingly, chronic GH pretreatment or IRS-2 knockdown impaired insulin-induced activation of Akt but did not affect GLUT4 translocation to plasma membrane. It is well established that insulin results in a robust activation of Akt that is in larger excess than required for GLUT4 translocation (42–44). Thus it is likely that a low level of Akt activation is sufficient for GLUT4 translocation, whereas greater Akt activity is required for activation of glucose uptake. In addition, it is also possible that appropriate subcellular localization of Akt activation is required to engage substrate required for GLUT4 activation. Previously, we reported that IRS-1 and IRS-2 are localized differently and thus altering the balance of Akt association with these docking proteins by chronic GH treatment could result in different substrate accessibilities. This disturbance would then account for the inability of activated Akt to phosphorylate Akt substrates essential for GLUT4 activation. Preliminary data suggest that chronic GH pretreatment suppressed insu-

Downloaded from www.jbc.org at HIROSHIMA UNIVERSITY, on February 20, 2010

lin-stimulated Akt activation and substrate phosphorylation in the plasma membrane fraction with relatively normal Akt activation in the low density microsome fraction, in which GLUT4 vesicle is enriched.[6] Identification of plasma membrane Akt substrates, whose phosphorylation is suppressed by chronic GH pretreatment, is one approach that may resolve the potential differential signaling pathways of IRS-1- and IRS-2-mediated Akt activation.

Although additional studies will be required to resolve these issues, our data clearly demonstrate that chronic GH pretreatment of adipocytes impairs GLUT4 glucose transport activity without affecting translocation to the plasma membrane. In addition, chronic GH pretreatment inhibits IRS-2-associated PI 3-kinase leading to an impairment of GLUT4 transport activity on the plasma membrane.

Acknowledgments—We thank Dr. Takaaki Aoyagi (Institute of Microbial Chemistry, Tokyo, Japan) for leupeptin and pepstatin. We acknowledge the helpful discussion with Dr. Asako Takenaka (Meiji University, Kanagawa, Japan), and we thank Dr. Susan H. Hall (School of Medicine, University of North Carolina, Chapel Hill) for the help in preparing this manuscript.

REFERENCES

1. Bryant, N. J., Govers, R., and James, D. E. (2002) *Nat. Rev. Mol. Cell Biol.* **3,** 267–277
2. Ducluzeau, P. H., Fletcher, L. M., Vidal, H., Laville, M., and Tavare, J. M. (2002) *Diabetes Metab.* **28,** 85–92
3. Watson, R. T., Kanzaki, M., and Pessin, J. E. (2004) *Endocr. Rev.* **25,** 177–204
4. Gronborg, M., Wulff, B. S., Rasmussen, J. S., Kjeldsen, T., and Gammeltoft, S. (1993) *J. Biol. Chem.* **268,** 23435–23440
5. Ullrich, A., and Schlessinger, J. (1990) *Cell* **61,** 203–212
6. Skolnik, E. Y., Lee, C. H., Batzer, A., Vicentini, L. M., Zhou, M., Daly, R., Myers, M. J., Jr., Backer, J. M., Ullrich, A., White, M. F., and Schlessinger, J. (1993) *EMBO J.* **12,** 1929–1936
7. White, M. F. (1997) *Diabetologia* **40,** Suppl. 2, 2–17
8. Backer, J. M., Myers, M. G., Jr., Shoelson, S. E., Chin, D. J., Sun, X. J., Miralpeix, M., Hu, P., Margolis, B., Skolnik, E. Y., Schlessinger, J., and White, M. F. (1992) *EMBO J.* **11,** 3469–3479
9. White, M. F. (2002) *Am. J. Physiol.* **283,** E413–E422
10. Cheatham, B., Vlahos, C. J., Cheatham, L., Wang, L., Blenis, J., and Kahn, C. R. (1994) *Mol. Cell. Biol.* **14,** 4902–4911
11. Clarke, J. F., Young, P. W., Yonezawa, K., Kasuga, M., and Holman, G. D. (1994) *Biochem. J.* **300,** 631–635
12. Jiang, T., Sweeney, G., Rudolf, M. T., Klip, A., Traynor-Kaplan, A., and Tsien, R. Y. (1998) *J. Biol. Chem.* **273,** 11017–11024
13. Kotani, K., Carozzi, A. J., Sakaue, H., Hara, K., Robinson, L. J., Clark, S. F., Yonezawa, K., James, D. E., and Kasuga, M. (1995) *Biochem. Biophys. Res. Commun.* **209,** 343–348
14. Martin, S. S., Haruta, T., Morris, A. J., Klippel, A., Williams, L. T., and Olefsky, J. M. (1996) *J. Biol. Chem.* **271,** 17605–17608
15. Okada, T., Kawano, Y., Sakakibara, T., Hazeki, O., and Ui, M. (1994) *J. Biol. Chem.* **269,** 3568–3573
16. Sharma, P. M., Egawa, K., Huang, Y., Martin, J. L., Huvar, I., Boss, G. R., and Olefsky, J. M. (1998) *J. Biol. Chem.* **273,** 18528–18537
17. Galetic, I., Andjelkovic, M., Meier, R., Brodbeck, D., Park, J., and Hemmings, B. A. (1999) *Pharmacol. Ther.* **82,** 409–425
18. Sano, H., Kane, S., Sano, E., Miinea, C. P., Asara, J. M., Lane, W. S., Garner, C. W., and Lienhard, G. E. (2003) *J. Biol. Chem.* **278,** 14599–14602
19. Sano, H., Eguez, L., Teruel, M. N., Fukuda, M., Chuang, T. D., Chavez, J. A., Lienhard, G. E., and McGraw, T. E. (2007) *Cell Metab.* **5,** 293–303
20. Beck, P., Schalch, D. S., Parker, M. L., Kipnis, D. M., and Daughaday, W. H. (1965) *J. Lab. Clin. Med.* **66,** 366–379
21. Cerasi, E., and Luft, R. (1964) *Lancet* **2,** 769–771
22. Yuen, K., Cook, D., Ong, K., Chatelain, P., Fryklund, L., Gluckman, P., Ranke, M. B., Rosenfeld, R., and Dunger, D. (2002) *Clin. Endocrinol.* **57,** 333–341
23. Cho, Y., Ariga, M., Uchijima, Y., Kimura, K., Rho, J. Y., Furuhata, Y., Hakuno, F., Yamanouchi, K., Nishihara, M., and Takahashi, S. (2006) *Endocrinology* **147,** 5374–5384
24. Takano, A., Haruta, T., Iwata, M., Usui, I., Uno, T., Kawahara, J., Ueno, E., Sasaoka, T., and Kobayashi, M. (2001) *Diabetes* **50,** 1891–1900
25. Ariga, M., Nedachi, T., Akahori, M., Sakamoto, H., Ito, Y., Hakuno, F., and Takahashi, S. (2000) *Biochem. J.* **348,** 409–416
26. Hakuno, F., Kurihara, S., Watson, R. T., Pessin, J. E., and Takahashi, S. (2007) *J. Biol. Chem.* **282,** 37747–37758
27. Elmendorf, J. S., Chen, D., and Pessin, J. E. (1998) *J. Biol. Chem.* **273,** 13289–13296
28. Hare, J. F., and Lee, E. (1989) *Biochemistry* **28,** 574–580
29. Ross, S. A., Scott, H. M., Morris, N. J., Leung, W. Y., Mao, F., Lienhard, G. E., and Keller, S. R. (1996) *J. Biol. Chem.* **271,** 3328–3332
30. Sasson, S., Kaiser, N., Dan-Goor, M., Oron, R., Koren, S., Wertheimer, E., Unluhizarci, K., and Cerasi, E. (1997) *Diabetologia* **40,** 30–39
31. Nedachi, T., Akahori, M., Ariga, M., Sakamoto, H., Suzuki, N., Umesaki, K., Hakuno, F., and Takahashi, S. I. (2000) *Endocrinology* **141,** 2429–2438
32. Sakoda, H., Ogihara, T., Anai, M., Funaki, M., Inukai, K., Katagiri, H., Fukushima, Y., Onishi, Y., Ono, H., Fujishiro, M., Kikuchi, M., Oka, Y., and Asano, T. (2000) *Diabetes* **49,** 1700–1708
33. Miyake, S., Makimura, M., Kanegae, Y., Harada, S., Sato, Y., Takamori, K., Tokuda, C., and Saito, I. (1996) *Proc. Natl. Acad. Sci. U. S. A.* **93,** 1320–1324
34. Scheepers, A., Joost, H. G., and Schurmann, A. (2004) *JPEN J. Parenter. Enteral. Nutr.* **28,** 364–371
35. Watson, R. T., and Pessin, J. E. (2001) *Recent Prog. Horm. Res.* **56,** 175–193
36. Sweeney, G., Keen, J., Somwar, R., Konrad, D., Garg, R., and Klip, A. (2001) *Endocrinology* **142,** 4806–4812
37. Nelson, B. A., Robinson, K. A., and Buse, M. G. (2000) *Diabetes* **49,** 981–991
38. Smith, R. M., Tiesinga, J. J., Shah, N., Smith, J. A., and Jarett, L. (1993) *Arch. Biochem. Biophys.* **300,** 238–246
39. Funaki, M., Randhawa, P., and Janmey, P. A. (2004) *Mol. Cell. Biol.* **24,** 7567–7577
40. Huang, C., Thirone, A. C., Huang, X., and Klip, A. (2005) *J. Biol. Chem.* **280,** 19426–19435
41. Kabuta, T., Hakuno, F., Asano, T., and Takahashi, S. (2002) *J. Biol. Chem.* **277,** 6846–6851
42. Guilherme, A., and Czech, M. P. (1998) *J. Biol. Chem.* **273,** 33119–33122
43. Kim, Y. B., Nikoulina, S. E., Ciaraldi, T. P., Henry, R. R., and Kahn, B. B. (1999) *J. Clin. Investig.* **104,** 733–741
44. Venable, C. L., Frevert, E. U., Kim, Y. B., Fischer, B. M., Kamatkar, S., Neel, B. G., and Kahn, B. B. (2000) *J. Biol. Chem.* **275,** 18318–18326

[6] T. Ogata, K. Kasahara, F. Hakuno, and S.-I. Takahashi, unpublished data.

Downloaded from www.jbc.org at HIROSHIMA UNIVERSITY, on February 20, 2010

Am J Physiol Endocrinol Metab 296: E157–E164, 2009.
First published November 11, 2008; doi:10.1152/ajpendo.90581.2008.

Impact of lipid phosphatases SHIP2 and PTEN on the time- and Akt-isoform-specific amelioration of TNF-α-induced insulin resistance in 3T3-L1 adipocytes

Mariko Ikubo,[1] Tsutomu Wada,[2] Kazuhito Fukui,[1] Manabu Ishiki,[1] Hajime Ishihara,[3] Tomoichiro Asano,[4] Hiroshi Tsuneki,[2] and Toshiyasu Sasaoka[2]

[1]*Department of Internal Medicine and* [2]*Department of Clinical Pharmacology, University of Toyama;* [3]*Sainou South Hospital, Toyama; and* [4]*Division of Molecular Medical Science, Hiroshima University, Hiroshima, Japan*

Submitted 10 July 2008; accepted in final form 4 November 2008

Ikubo M, Wada T, Fukui K, Ishiki M, Ishihara H, Asano T, Tsuneki H, Sasaoka T. Impact of lipid phosphatases SHIP2 and PTEN on the time- and Akt-isoform-specific amelioration of TNF-α-induced insulin resistance in 3T3-L1 adipocytes. *Am J Physiol Endocrinol Metab* 296: E157–E164, 2009. First published November 11, 2008; doi:10.1152/ajpendo.90581.2008.—TNF-α is a major contributor to the pathogenesis of insulin resistance associated with obesity and inflammation by serine phosphorylating and degrading insulin receptor substrate-1. Presently, we further found that pretreatment with TNF-α inhibited insulin-induced phosphorylation of Akt2 greater than Akt1. Since lipid phosphatases SH2-containing inositol 5′-phoshatase 2 (SHIP2) and phosphatase and tensin homologs deleted on chromosome 10 (PTEN) are negative regulators of insulin's metabolic signaling at the step downstream of phosphatidylinositol 3-kinase, we investigated the Akt isoform-specific properties of these phosphatases in the negative regulation after short- and long-term insulin treatment and examined the influence of inhibition on the amelioration of insulin resistance caused by TNF-α in 3T3-L1 adipocytes. Adenovirus-mediated overexpression of WT-SHIP2 decreased the phosphorylation of Akt2 greater than Akt1 after insulin stimulation up to 15 min. Expression of a dominant-negative ΔIP-SHIP2 enhanced the phosphorylation of Akt2 up to 120 min. On the other hand, overexpression of WT-PTEN inhibited the phosphorylation of both Akt1 and Akt2 after short- but not long-term insulin treatment. The expression of ΔIP-PTEN enhanced the phosphorylation of Akt1 at 120 min and that of Akt2 at 2 min. Interestingly, the expression of ΔIP-SHIP2, but not ΔIP-PTEN, protected against the TNF-α inhibition of insulin-induced phosphorylation of Akt2, GSK3, and AS160, whereas both improved the TNF-α inhibition of insulin-induced 2-deoxyglucose uptake. The results indicate that these lipid phosphatases possess different characteristics according to the time and preference of Akt isoform-dependent signaling in the negative regulation of the metabolic actions of insulin, whereas both inhibitions are effective in the amelioration of insulin resistance caused by TNF-α.

insulin signaling; SH2-containing inositol 5′-phoshatase 2; phosphatase and tensin homologs deleted on chromosome 10

THE ACTIVATED INSULIN RECEPTOR phosphorylates insulin receptor substrates (IRS) at tyrosine residues (17, 26, 28). The tyrosine phosphorylated IRS binds to the regulatory subunit of phosphatidylinositol 3-kinase (PI3-kinase), which in turn activates the p110 catalytic subunit (3, 32, 36). The activation of PI3-kinase is known to be important for the various metabolic actions of insulin (3, 33, 37). PI3-kinase functions as a lipid kinase to produce $PI(3,4,5)P_3$ from $PI(4,5)P_2$ in vivo (32). $PI(3,4,5)P_3$ acts as a key lipid second messenger in insulin signaling to further downstream molecules, including Akt (30, 38). Lipid phosphatases were identified to hydrolyze $PI(3,4,5)P_3$ in the negative regulation of insulin signaling (12, 20, 25). SH2-containing inositol 5′-phoshatase 2 (SHIP2) functions as a lipid phosphatase possessing 5′-phosphatase activity to hydrolyze $PI(3,4,5)P_3$ to $PI(3,4)P_2$ (38). Phosphatase and tensin homologs deleted on chromosome 10 (PTEN) act as a 3′-lipid phosphatase hydrolyzing $PI(3,4,5)P_3$ to $PI(4,5)P_2$ (20). Targeted disruption of the SHIP2 gene in mice resulted in increased insulin sensitivity and conferred protection against obesity induced by a high-fat diet (4, 33). Since homozygous disruption of the PTEN gene in mice results in embryonic lethality, the tissue-specific role of PTEN was investigated (7). Liver, skeletal muscle, or adipose tissue-specific disruption of PTEN ameliorated glucose metabolism in the animal model of diabetes (18, 34, 39); therefore, lipid phosphatases, both SHIP2 and PTEN, appear to be implicated in glucose metabolism.

Adipocytes are important target tissues of insulin, and 3T3-L1 cells are well-characterized adipocytes (22, 23, 38). Overexpression of SHIP2 and PTEN is reported to inhibit insulin-induced phosphorylation of Akt and glucose uptake (22, 23, 38); however, the effect of SHIP2 and PTEN expression has been examined only after short-term insulin treatment with controversial results (23, 35). In addition, the role of these lipid phosphatases in the regulation of metabolic signaling after long-term insulin treatment is unknown; therefore, it would be of particular importance to clarify the possible differences in characteristics and properties among these lipid phosphatases to further understand the molecular mechanism of the negative regulation of insulin signaling.

Akt is one of the downstream target molecules of PI3-kinase important for glucose metabolism (5, 6, 38). Akt1 and Akt2 are the isoforms mainly expressed in adipocytes (31, 38). Studies (5, 6) with Akt1 and Akt2 knockout mice revealed that Akt2 is preferentially implicated in glucose metabolism, whereas Akt1 is mainly involved in cell growth. The comparative effect of SHIP2 and PTEN on short- and long-term insulin-induced phosphorylation of Akt1 and Akt2 is uncertain in 3T3-L1 adipocytes. In addition, TNF-α is an important cytokine implicated in the development of insulin resistance in type 2 diabetes (14, 27, 39); therefore, investigation of the ameliorative effect by inhibition of these endogenous lipid phosphatases

Address for reprint requests and other correspondence: T. Sasaoka, Dept. of Clinical Pharmacology, Univ. of Toyama, 2630 Sugitani, Toyama 930-0194, Japan (e-mail: tsasaoka@pha.u-toyama.ac.jp).

The costs of publication of this article were defrayed in part by the payment of page charges. The article must therefore be hereby marked "*advertisement*" in accordance with 18 U.S.C. Section 1734 solely to indicate this fact.

0193-1849/09 $8.00 Copyright © 2009 the American Physiological Society

Downloaded from ajpendo.physiology.org on February 20, 2010

on TNF-α-induced insulin resistance is important to clarify the therapeutic value in type 2 diabetes.

In the present study, we directly compared the role of lipid phosphatases SHIP2 and PTEN in short- and long-term insulin-induced phosphorylation of Akt1 and Akt2 in 3T3-L1 adipocytes. Furthermore, we investigated whether the inhibition of endogenous SHIP2 and PTEN by phosphatase-defective mutant expression protects against the impairment of insulin-induced phosphorylation of Akt, GSK3, and Akt substrate 160 (AS160), and glucose uptake by pretreatment with TNF-α.

MATERIALS AND METHODS

Materials. Human crystal insulin was provided by Novo Nordisk Pharmaceutical (Copenhagen, Denmark). 2-[^{3}H]deoxyglucose (2DG; 3,330 GBq/mM) was purchased from NEN Life Science Products (Boston, MA). Human recombinant TNF-α was obtained from Pepro Tech (Rocky Hill, NJ). The two polyclonal anti-SHIP2 antibodies were described previously (12). A monoclonal anti-phosphotyrosine antibody (PY20) was purchased from Transduction Laboratories (Lexington, KY). A polyclonal anti-Thr$^{308/309}$ phospho-specific Akt antibody and a polyclonal anti-Ser$^{473/474}$ phospho-specific Akt antibody, a polyclonal anti-Akt antibody, a polyclonal anti-Akt2 antibody, a polyclonal anti-Ser$^{21/9}$ phospho-specific GSK3α/β antibody, a polyclonal anti-GSK3α/β antibody, an a polyclonal anti-Ser/Thr-phospho-specific Akt substrate antibody, and a polyclonal anti-AS160 antibody were from Cell Signaling (Beverly, MA). A monoclonal anti-Akt1 antibody and a monoclonal anti-PTEN antibody were from Santa Cruz Biotechnology (Santa Cruz, CA). A polyclonal anti-IRS-1 antibody was from Upstate Biotechnology (Lake Placid, NY). Enhanced chemiluminescence reagents were from GE Healthcare Bio-Science (Tokyo, Japan). DMEM was from GIBCO-BRL Japan (Tokyo, Japan). All other reagents were of analytical grade and purchased from Sigma Chemical (St. Louis, MO) or Wako Pure Chemical Industries (Osaka, Japan).

Adenoviral vectors. Adenoviral vectors encoding wild-type SHIP2 (WT-SHIP2), a phosphatase-defective mutant SHIP2 (ΔIP-SHIP2) containing Pro^{687} to Ala, Asp^{691} to Ala, and Arg^{692} to Gly changes (38), wild-type PTEN (WT-PTEN), and a phosphatase-defective mutant PTEN (ΔIP-PTEN) containing Cys^{124} to Ser change (23) were described previously.

Cell culture and infections with adenovirus. 3T3-L1 fibroblasts were grown and passaged in DMEM supplemented with 10% donor calf serum. Cells at 2–3 days postconfluence were used for differentiation. The differentiation medium contained 10% FBS, 250 nM dexamethazone, 0.5 mM IBMX, and 500 nM insulin. After 3 days, the differentiation medium was replaced with postdifferentiation medium containing 10% FBS and 500 nM insulin. After 3 more days, the postdifferentiation medium was replaced with DMEM including 25 mM glucose supplemented with 10% FBS. SHIP2 and PTEN were transiently expressed in differentiated 3T3-L1 adipocytes by means of adenovirus-mediated gene transfer. A multiplicity of infection (MOI) of 10–40 plaque-forming units (PFU)/cell was used to infect 3T3-L1 adipocytes in DMEM containing 2% FBS, with the virus being left on the cells for 16 h before removal. Subsequent experiments were conducted 24–48 h after initial addition of the virus (38). The efficiency of adenovirus-mediated gene transfer of SHIP2 and PTEN was ~95%.

Insulin and TNF-α treatment. 3T3-L1 adipocytes grown in six-well multiplates were incubated with DMEM containing 0.1% FBS without or with 17 nM insulin at 37°C for 2- to 120-min periods. For experiments with TNF-α treatment, 20 nM TNF-α were added for 16 h and then treated with 17 nM insulin for 10 or 120 min.

Immunoprecipitation and Western blotting. The cells were lysed in a buffer containing 20 mM Tris, 150 mM NaCl, 1 mM EDTA, 1 mM EGTA, 2.5 mM sodium deoxycholate, 1 mM β-glycerophosphate, 1% NP40, 1 mM PMSF, 1 mM Na_3VO_4, 50 mM sodium fluoride, 10 μg/ml of aprotinin, and 10 μM leupeptin, pH 7.4, for 30 min at 4°C. The lysates were centrifuged to remove insoluble materials. The supernatants (100 μg of protein) were immunoprecipitated with antibodies for 2 h at 4°C. The precipitates or the lysates were then separated by 7.5% SDS-PAGE and transferred onto polyvinylidene difluoride membranes using a Bio-Rad Transblot apparatus. The membranes were blocked in a buffer containing 50 mM Tris, 150 mM NaCl, 0.1% Tween 20, and 2.5% BSA or 5% nonfat milk, pH 7.5, for 2 h at 20°C. They were then probed with antibodies for 2 h at 20°C or for 16 h at 4°C. After the membranes were washed in a buffer containing 50 mM Tris, 150 mM NaCl, and 0.1% Tween 20, pH 7.5, the blots were incubated with a horseradish peroxidase-linked secondary antibody and subjected to enhanced chemiluminescence detection using ECL reagent according to the manufacturer's instructions (GE Health Science Bio-Science; Ref. 38). Densitometric analysis was conducted directly from the blotted membrane by utilizing LAS-4000 lumino-image analyzer system (Fujifilm, Tokyo, Japan). The relative phosphorylation level of each protein was calculated as the ratio of phosphorylated to total protein level.

Measurement of 2-deoxyglucose uptake. 3T3-L1 adipocytes grown in six-well multiplates were pretreated with TNF-α and serum starved for 2 h. The cells were washed twice with PBS and incubated with Krebs-Ringer phosphate-HEPES buffer, 10 nM HEPES, 131.2 mM NaCl, 4.7 mM KCl, 1.2 mM $MgSO_4$, 2.5 mM $CaCl_2$, and 2.5 mM NaH_2PO_4, containing 1% BSA, pH 7.4, for 1 h at 37°C. The cells were subsequently stimulated with various concentrations of insulin. After a 15-min insulin treatment, 3.7 kBq of 2-[^{3}H]deoxyglucose (2-DG) were added for 4 min. The reaction was stopped by the addition of 10 μnol/l cytochalasin B. The cells were washed three times with PBS and solubilized with 0.2 mM SDS-0.2 N NaOH (38). The radioactivity incorporated into the cells was measured by liquid scintillation counting.

Statistical analysis. Data are expressed as means ± SE. P values were determined by one-way ANOVA with Bonferroni's correction test, and $P < 0.05$ was considered significant.

RESULTS

Expression of lipid phosphatases in 3T3-L1 adipocytes. SHIP2 (140-kDa) is a 5′-lipid phosphatase and PTEN (54-kDa) is a 3′-lipid phosphatase, both of which are known to be involved in the negative regulation of insulin signaling (22, 23, 30, 38). Endogenous SHIP2 and PTEN were clearly observed in control 3T3-L1 adipocytes. Consensus amino acids located within the catalytic domain of lipid phosphatases were mutated to generate phosphatase-defective SHIP2 (ΔIP-SHIP2) and PTEN (ΔIP-PTEN) (23, 38). Wild-type and phosphatase-defective lipid phosphatases were transiently expressed in 3T3-L1 adipocytes by means of adenovirus-mediated gene transfer. By transfecting with these lipid phosphatase genes at an MOI of 10 PFU/cell (Fig. 1, *A* and *B*) and 40 PFU/cell (Fig. 1, *C* and *D*), we observed a 2.5- and 5-fold increase in expression levels of SHIP2 and a 4- and 7-fold increase in expression levels of PTEN, respectively, over the endogenous level in 3T3-L1 adipocytes. Since the obtained results with expression at an MOI of 10 and 40 PFU/cell were similar, the after analyses were shown at an MOI of 40 PFU/cell.

Effect of expression of wild-type lipid phosphatases on insulin-induced phosphorylation of Akt. Akt is one of the downstream target molecules of PI3-kinase and has been shown to mediate the metabolic actions of insulin (5, 38). We compared the effect of WT-SHIP2 and WT-PTEN expressions on the phosphorylation of Akt1 and Akt2 after insulin stimulation for up to 120 min in 3T3-L1 adipocytes. Overexpression

Downloaded from ajpendo.physiology.org on February 20, 2010

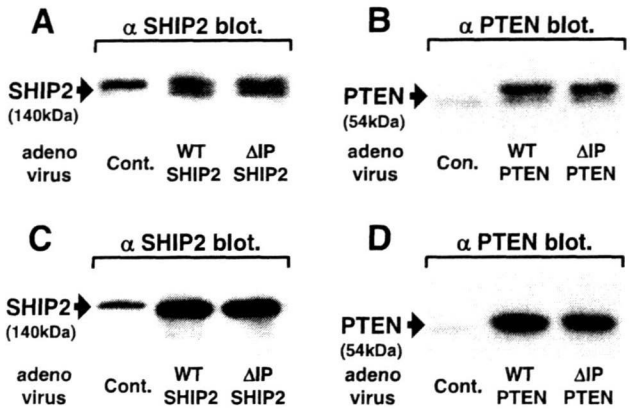

Fig. 1. Expression of lipid phosphatases in 3T3-L1 adipocytes. 3T3-L1 adipocytes were transfected with LacZ, wild-type SH2-containing inositol 5′-phosphatase 2 (WT-SHIP2), phosphatase-defective mutant SHIP2 (ΔIP-SHIP2), wild-type phosphatase and tensin homologs deleted on chromosome 10 (WT-PTEN), and ΔIP-PTEN at a multiplicity of infection (MOI) of 10 plaque-forming units (PFU)/cells (*A* and *B*) and 40 PFU/cells (*C* and *D*). After infection, cells were lysed and subjected to immunoblot analysis with anti-SHIP2 antibody (*A* and *C*) and anti-PTEN antibody (*B* and *D*). Results represent 3 separate experiments.

of WT-SHIP2 mildly inhibited the phosphorylation of Akt1 at Thr^{308} after insulin stimulation for up to 120 min (13.0% reduction at 5 min; Fig. 2*A*). On the other hand, overexpression of WT-SHIP2 greatly inhibited Akt2 phosphorylation at Thr^{309} after insulin treatment for up to 15 min (30.9% reduction at 5 min; Fig. 2*C*). Overexpression of WT-PTEN significantly inhibited insulin-induced Akt1 phosphorylation at 2 and 5 min by 26.6 and 16.5%, respectively (Fig. 2*B*). Insulin-induced phosphorylation of Akt2 at 2 and 5 min was also inhibited by 29.1 and 20.0%, respectively, by the overexpression of WT-PTEN (Fig. 2*D*). Similar results were obtained concerning Akt phosphorylation at $Ser^{473/474}$ residue and GSK3 phosphorylation at $Ser^{21/9}$ residue (data not shown).

Effect of expression of phosphatase-defective (ΔIP) lipid phosphatases on insulin-induced phosphorylation of Akt. Expression of ΔIP-SHIP2 enhanced Akt1 phosphorylation at Thr^{308}, and phosphorylation was significantly enhanced by 70.4% after 120 min of insulin treatment (Fig. 3*A*). The enhancing effect was more apparent in Akt2 phosphorylation at Thr^{309}. Phosphorylation of Akt2 at 2, 5, and 120 min of insulin treatment was significantly augmented by 20.7, 16.6, and 93.7%, respectively, by the expression of ΔIP-SHIP2 (Fig. 3*C*). Expression of ΔIP-PTEN enhanced long-term insulin-stimulated Akt1 phosphorylation, which was significantly augmented by 43.9% after 120 min of insulin treatment (Fig. 3*B*). Phosphorylation of Akt2 at only 2 min of insulin stimulation was slightly enhanced by 17.7% by the expression of ΔIP-PTEN (Fig. 3*D*). Similar results were again obtained concerning the phosphorylation of Akt at $Ser^{473/474}$ residue and GSK3 at $Ser^{21/9}$ residue (data not shown).

Expression of phosphatase-defective lipid phosphatases ameliorates insulin-induced phosphorylation of Akt after TNF-α treatment. We next examined the ameliorative effect of the expression of phosphatase-defective lipid phosphatases on the decreased insulin-induced phosphorylation of Akt by pre-

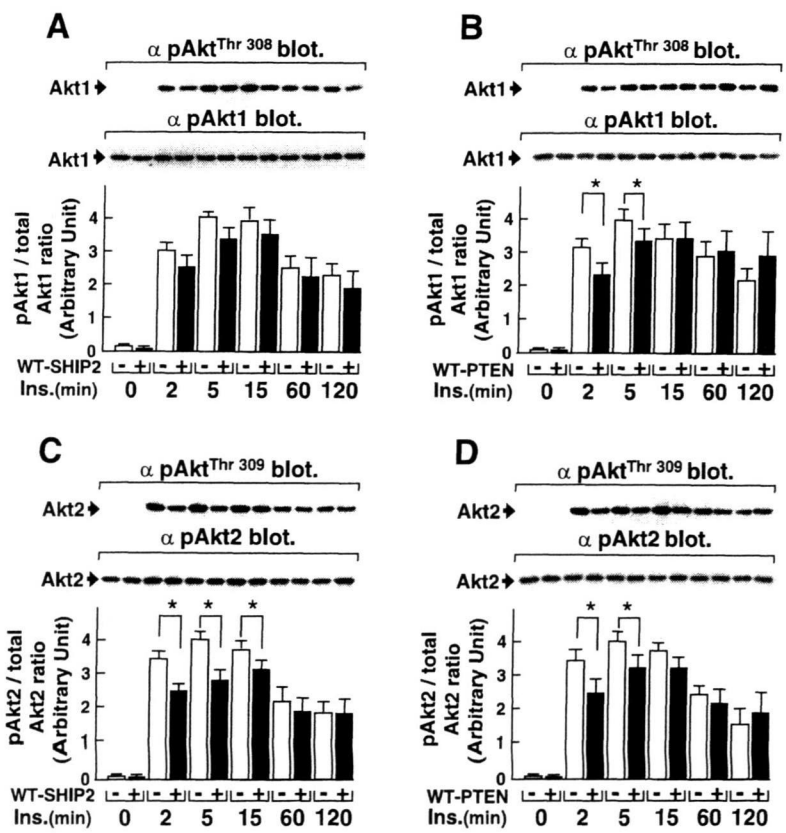

Fig. 2. Effect of wild-type SHIP2 and PTEN overexpression on insulin-induced phosphorylation of Akt. 3T3-L1 adipocytes were transfected with WT-SHIP2 (*A* and *C*) and WT-PTEN (*B* and *D*) at an MOI of 40 PFU/cell. Cells were serum starved for 16 h and subsequently treated with 17 nM insulin at 37°C for indicated times. Cells were immunoprecipitated with anti-Akt1 antibody (*A* and *B*) or anti-Akt2 antibody (*C* and *D*). Precipitates were separated by 7.5% SDS-PAGE and immunoblotted with anti-$Thr^{308/309}$-phospho-specific Akt antibody, anti-Akt1 antibody, or anti-Akt2 antibody. Amount of Akt phosphorylated at $Thr^{308/309}$ corrected for total protein level was quantitated by densitometry. Results are means ± SE of 5 separate experiments. *$P < 0.05$ vs. amount of phosphorylated Akt in LacZ-transfected cells with respective insulin treatment.

Downloaded from ajpendo.physiology.org on February 20, 2010

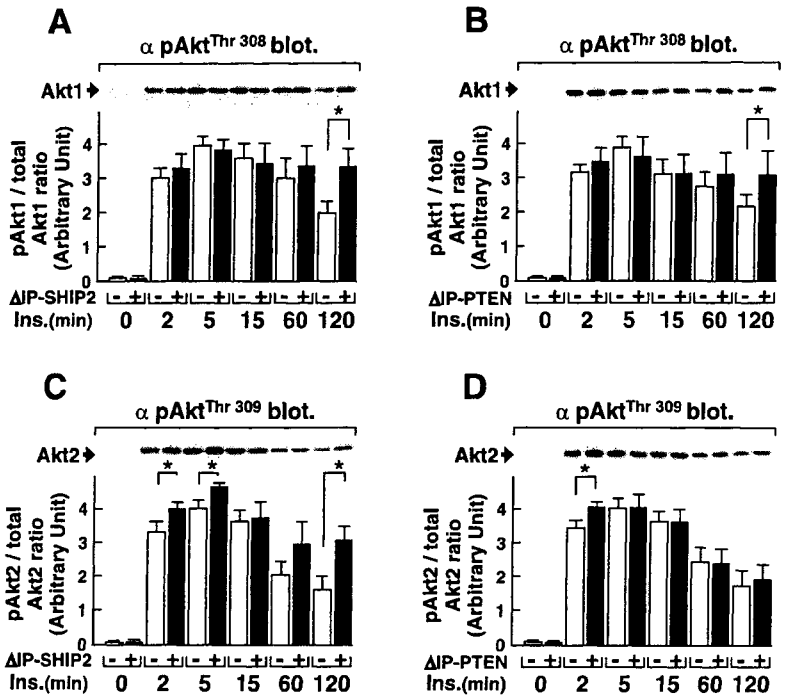

Fig. 3. Effect of phosphatase-defective SHIP2 and PTEN expression on insulin-induced phosphorylation of Akt. 3T3-L1 adipocytes were transfected with ΔIP-SHIP2 (*A* and *C*) and ΔIP-PTEN (*B* and *D*) at an MOI of 40 PFU/cell. Cells were serum starved for 16 h and subsequently treated with 17 nM insulin at 37°C for indicated times. Cells were immunoprecipitated with anti-Akt1 antibody (*A* and *B*) or anti-Akt2 antibody (*C* and *D*). Precipitates were separated by 7.5% SDS-PAGE and immunoblotted with anti-$Thr^{308/309}$-phospho-specific Akt antibody. Amount of Akt phosphorylated at $Thr^{308/309}$ corrected for total protein level was quantitated by densitometry. Results are means ± SE of 5 separate experiments. $*P < 0.05$ vs. amount of phosphorylated Akt in LacZ-transfected cells with respective insulin (Ins.) treatment.

treatment with TNF-α (Fig. 4). Pretreatment with TNF-α decreased the phosphorylation of Akt1 at Thr^{308} after insulin stimulation for 10 min (*lane 5* vs. *7*) but not for 120 min (*lane 9* vs. *11*). The TNF-α-induced decrease in insulin-induced phosphorylation of Akt1 at 10 min was not apparently affected by the expression of either ΔIP-SHIP2 (Fig. 4*A*) or ΔIP-PTEN (Fig. 4*B*). In contrast, the expression of either phosphatase-defective mutant enhanced insulin-induced phosphorylation of Akt1 at 120 min even after pretreatment with TNF-α (Fig. 3, *A* and *B*, and Fig. 4, *A* and *B*). On the other hand, pretreatment with TNF-α markedly inhibited the insulin-induced phosphorylation of Akt2 (Thr^{309} residue) at 10 min (*lane 5* vs. *7*) and also at 120 min (*lane 9* vs. *11*). The decreased phosphorylation of Akt2 by pretreatment with TNF-α was effectively ameliorated by the expression of ΔIP-SHIP2 (Fig. 4*C*) but not by the expression of ΔIP-PTEN (Fig. 4*D*). Similar results were ob-

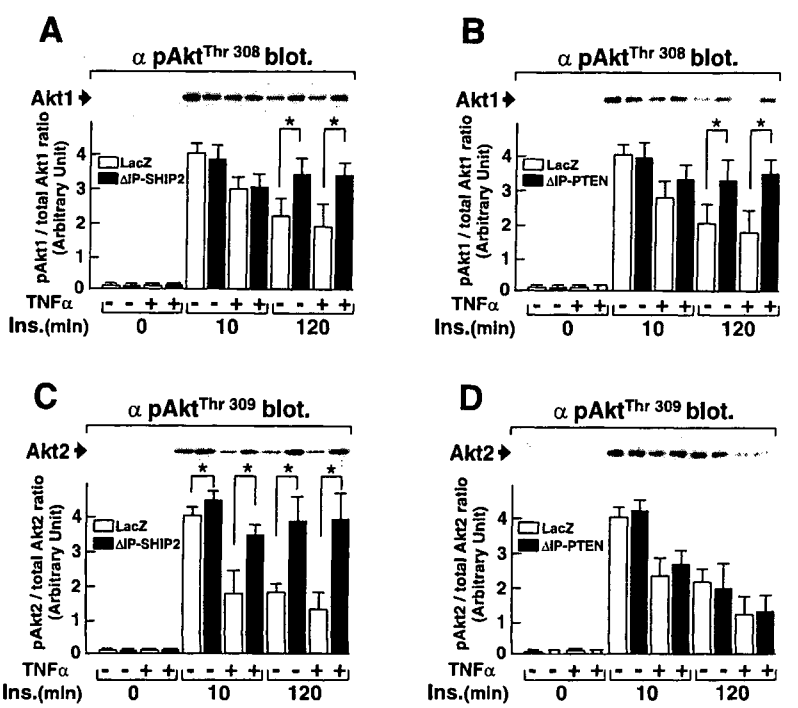

Fig. 4. Effect of phosphatase-defective SHIP2 and PTEN expression on TNF-α-induced decrease in phosphorylation of Akt. 3T3-L1 adipocytes were transfected with ΔIP-SHIP2 (*A* and *C*) and ΔIP-PTEN (*B* and *D*) at an MOI of 40 PFU/cell. Serum-starved transfected cells preincubated with 20 nM TNF-α for 16 h were treated with 17 nM insulin for 10 and 120 min. Cells were immunoprecipitated with anti-Akt1 antibody (*A* and *B*) or anti-Akt2 antibody (*C* and *D*). Precipitates were separated by 7.5% SDS-PAGE and immunoblotted with anti-$Thr^{308/309}$-phospho-specific Akt antibody. Amount of phosphorylated Akt at $Thr^{308/309}$ corrected for total protein level was quantitated by densitometry. Results are means ± SE of 4 separate experiments. $*P < 0.05$ vs. amount of phosphorylated Akt in LacZ-transfected cells with respective insulin treatment.

Downloaded from ajpendo.physiology.org on February 20, 2010

tained by the reciprocal immunoblotting studies with anti-Akt1 antibody or anti-Akt2 antibody after immunoprecipitation with anti-Thr$^{308/309}$ phospho-specific Akt antibody (data not shown). In addition, similar findings were again observed concerning the phosphorylation of Akt at Ser$^{473/474}$ residue (data not shown).

Expression of phosphatase-defective lipid phosphatases ameliorates insulin-induced phosphorylation of GSK3 and AS160 after TNF-α treatment. GSK3 and AS160 are important downstream molecules of Akt implicated in the metabolic action of insulin (3, 28, 37). We therefore investigated the ameliorative effect of the expression of phosphatase-defective lipid phosphatases on the decreased insulin-induced phosphorylation of GSK3 and AS160 by pretreatment with TNF-α (Fig. 5). Pretreatment with TNF-α decreased the phosphorylation of GSK3 and AS160 after insulin stimulation for 10 min (*lane 5* vs. *7*) and for 120 min (*lane 9* vs. *11*). TNF-α-induced decrease in insulin-induced phosphorylation of both GSK3 and AS160 was relatively more ameliorated by the expression of ΔIP-SHIP2 (Fig. 5, *A* and *C*) than that of ΔIP-PTEN (Fig. 5, *B* and *D*). These results indicate that the change of GSK3 and AS160 phosphorylations is relatively correlated with the phosphorylation of Akt2 rather than Akt1 by the expression of ΔIP-SHIP2.

Expression of phosphatase-defective lipid phosphatases does not affect insulin-induced degradation and tyrosine phosphorylation of IRS-1 after TNF-α treatment. We further examined whether expression of phosphatase-defective lipid phosphatases affects insulin-induced degradation and tyrosine phosphorylation of IRS-1 after TNF-α treatment, since TNF-α is an important adipokine that causes insulin resistance by facilitating the degradation of IRS-1 in 3T3-L1 adipocytes (14). As a result, insulin-induced tyrosine phosphorylation of IRS-1 is decreased after pretreatment with TNF-α (14). Consistent with these findings, pretreatment with TNF-α caused the degradation of IRS-1, and the subsequent tyrosine phosphorylation of IRS-1 after insulin treatment for 10 and 120 min was decreased. The expression of neither ΔIP-SHIP2 (Fig. 6*A*) nor ΔIP-PTEN (Fig. 6*B*) affected TNF-α- and insulin-induced degradation of IRS-1. Similarly, the suppressing effect of TNF-α on insulin-induced tyrosine phosphorylation of IRS-1 at 10 and 120 min was not affected by the expression of either ΔIP-SHIP2 (Fig. 6*C*) or ΔIP-PTEN (Fig. 6*D*). These results indicate that the expression of ΔIP-SHIP2 and ΔIP-PTEN ameliorates the decreased Akt-dependent signaling without affecting degradation of IRS-1. It is of note that treatment with TNF-α itself also did not affect the expression of endogenous SHIP2 and PTEN (data not shown).

Effect of expression of phosphatase-defective lipid phosphatases on insulin-induced glucose uptake after TNF-α treatment. We finally examined the effect of the expression of phosphatase-defective lipid phosphatases on insulin-induced 2-DG uptake in the presence or absence of TNF-α (Fig. 7). The expression of either ΔIP-SHIP2 or ΔIP-PTEN enhanced insulin-induced 2-DG uptake, although the former augmented it greater than the latter. Treatment with TNF-α inhibited 1.7- and 17-nM insulin-induced 2-DG uptake by 42.7 and 19.0%,

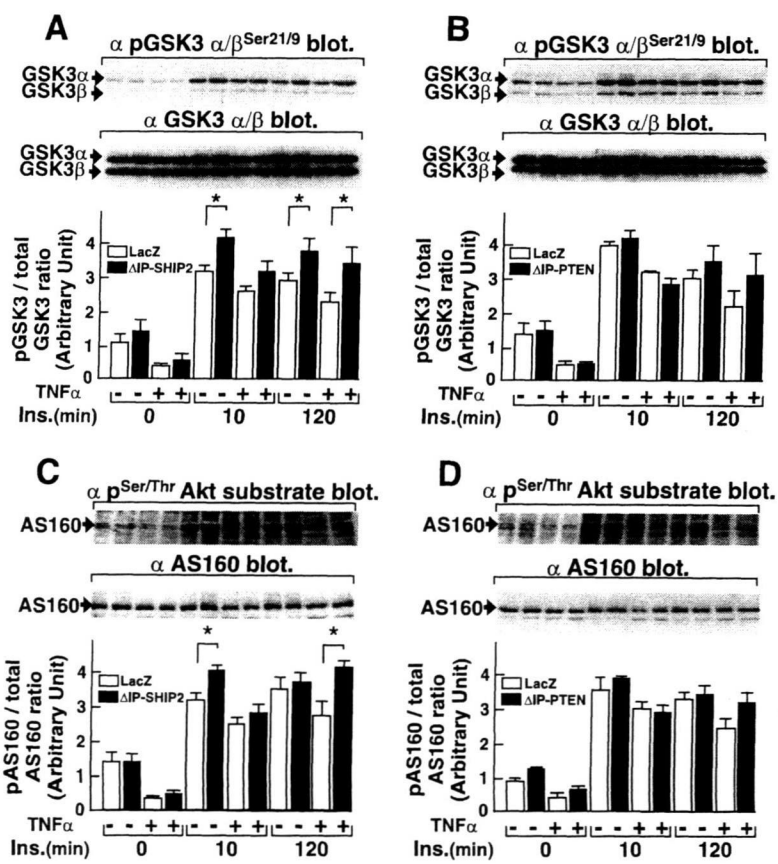

Fig. 5. Effect of phosphatase-defective SHIP2 and PTEN expression on TNF-α-induced decrease in phosphorylation of GSK3 and AS160. 3T3-L1 adipocytes were transfected with ΔIP-SHIP2 (*A* and *C*) and ΔIP-PTEN (*B* and *D*) at an MOI of 40 PFU/cell. Serum-starved transfected cells preincubated with 20 nM TNF-α for 16 h were treated with 17 nM insulin for 10 and 120 min. Total cell lysates were separated by 7.5% SDS-PAGE and immunoblotted with anti-Ser$^{21/9}$-phospho-specific GSK3α/β antibody (*A* and *B*), anti-GSK3α/β antibody (*A* and *B*), anti-Ser/Thr-phospho-specific Akt substrate antibody (*C* and *D*), or anti-AS160 antibody (*C* and *D*). Amount of phosphorylated GSK3 and AS160 corrected for total GSK3 and AS160 levels, respectively, was quantitated by densitometry. Results are expressed as means ± SE of 4 separate experiments. *P < 0.05 vs. amount of phosphorylated GSK3 or AS160 in LacZ-transfected cells with respective insulin treatment.

Downloaded from ajpendo.physiology.org on February 20, 2010

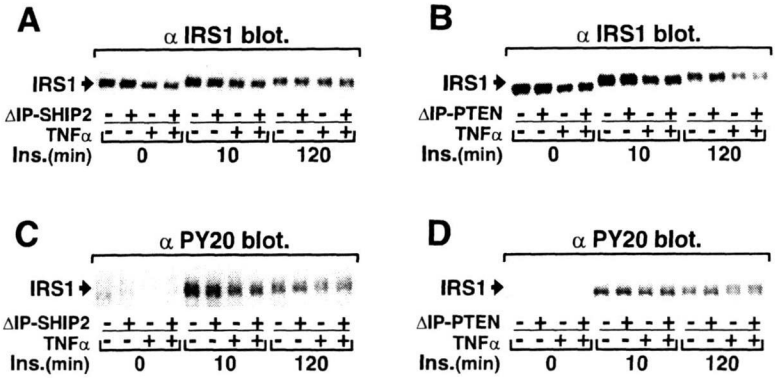

Fig. 6. Effect of phosphatase-defective SHIP2 and PTEN expression on insulin-induced degradation and tyrosine phosphorylation of IRS-1 after pretreatment with TNF-α. 3T3-L1 adipocytes were transfected with ΔIP-SHIP2 (*A* and *C*) and ΔIP-PTEN (*B* and *D*) at an MOI of 40 PFU/cell. Cells were serum starved for 16 h and subsequently pretreated with 20 ng/ml of TNF-α for 16 h. They were then treated with 17 nM insulin at 37°C for 10 and 120 min. Cells were lysed and separated by 7.5% SDS-PAGE and immunoblotted with anti-IRS-1 antibody (*A* and *B*) or anti-phosphotyrosine antibody (*C* and *D*). Amount of IRS protein and tyrosine-phosphorylated IRS-1 was quantitated by densitometry. Results are means ± SE of 4 separate experiments. $*P < 0.05$ vs. amount of IRS in LacZ-transfected cells with respective insulin treatment.

respectively. Interestingly, the expression of either ΔIP-SHIP2 or ΔIP-PTEN ameliorated the reduced 2-DG uptake by pretreatment with TNF-α to the control level. The amount of GLUT4 protein was not altered by treatment with TNF-α or the expression of both ΔIP-SHIP2 and ΔIP-PTEN (data not shown).

DISCUSSION

SHIP2 and PTEN are lipid phosphatases known to be involved in the negative regulation of insulin signaling in vivo and/or in vitro (4, 18, 20, 23, 33–35, 38, 39); however, the possible difference in characteristics and properties among these lipid phosphatases after short- vs. long-term insulin treatment is still unknown. Our previous reports (31) showed that SHIP2 predominantly regulates the phosphorylation of Akt2, but not Akt1, after short-term insulin treatment. Again, our current results showed that overexpression of WT-SHIP2 inhibited insulin-induced phosphorylation of Akt2 rather than Akt1 only after insulin treatment for up to 15 min. Interestingly, the effect was diminished after 60 and 120 min of insulin stimulation. Furthermore, the expression of ΔIP-SHIP2 enhanced insulin-induced phosphorylation of Akt2 after both short- and long-term insulin treatments, whereas phosphorylation of Akt1 was augmented only after 120 min of insulin treatment by the expression; therefore, the present results further clarified the characteristics of the regulation of insulin signaling by SHIP2, indicating that SHIP2 predominantly regulates the phosphorylation of Akt2 rather than Akt1 in a time-specific manner.

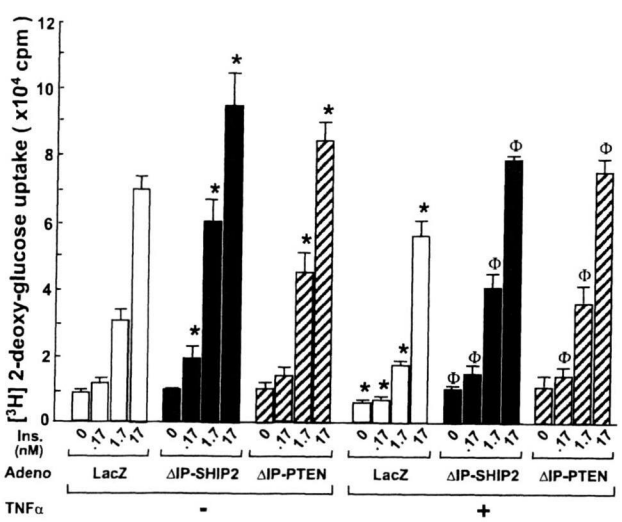

Fig. 7. Effect of phosphatase-defective SHIP2 and PTEN expression on TNF-α-induced inhibition of glucose uptake. 3T3-L1 adipocytes were transfected with ΔIP-SHIP2 or ΔIP-PTEN at an MOI of 40 PFU/cell. Serum-starved transfected cells pretreated with 20 nM TNF-α for 16 h were incubated in glucose-free medium for 30 min. After the cells had been stimulated with 10 nM insulin for 15 min, 3.7 kBq of 2-[^{3}H]deoxyglucose (2-[^{3}H]DG) were added for 4 min. Reaction was stopped by the addition of 10 μM cytochalasin B. Cells were washed 3 times with PBS and solubilized with 0.2 mM SDS-0.2 N NaOH. Radioactivity incorporated into the cells was measured with a liquid scintillation counter. Results are means ± SE of 5 separate experiments. $*P < 0.05$ vs. 2-[^{3}H]DG uptake in LacZ-transfected control cells with respective insulin treatment. $\Phi P < 0.05$ vs. 2-[^{3}H]DG uptake in TNF-α-treated cells with respective insulin treatment.

PTEN is a 3′-lipid phosphatase hydrolyzing PI(3,4,5)P_3 to PI(4,5)P_2 (20). It is reported that overexpression of WT-PTEN inhibited short-term insulin-induced activation of Akt, although the isoform-specific difference was not examined (22, 23, 35). On the other hand, the expression of ΔIP-PTEN did not affect short-term insulin-induced metabolic signaling, whereas the amount of PI(3,4,5)P_3 was increased in 3T3-L1 adipocytes (23). In contrast, depletion of PTEN protein by siRNA-mediated gene silencing enhanced short-term insulin-induced phosphorylation of Akt (35). The present studies showed that overexpression of WT-PTEN inhibited the phosphorylation of Akt1 and Akt2 after insulin stimulation for up to 5 min and that the effect was diminished thereafter. Our results clearly indicate that the effect of WT-PTEN expression is not specific to either Akt1 or Akt2 and is seen only after short-term insulin treatment. In addition, the expression of ΔIP-PTEN enhanced Akt2 phosphorylation, and only had a mild impact on augmenting the phosphorylation of Akt1 after 2 min of insulin treatment. Furthermore, ΔIP-PTEN expression enhanced the phosphorylation of Akt1, but not Akt2, after 120 min of insulin treatment. Taken together, PTEN appears to be implicated in the regulation of both short- and long-term insulin treatment-induced phosphorylation of Akt, whereas the Akt isoform-specific difference during regulation is ambiguous. SHIP2 is reported to translocate from cytosol to plasma membrane whereby phosphorylation of Akt2 is preferentially regulated upon insulin treatment (31), whereas the redistribution of PTEN is uncertain in 3T3-L1 adipocytes. The possible difference of subcellular redistribution between SHIP2 and PTEN may be a reason to cause an alteration in the isoform and temporal specific effects of Akt phosphorylation. Alternatively, it is possible that the stronger effect of SHIP2 on Akt2 and the

Downloaded from ajpendo.physiology.org on February 20, 2010

equivalent effects of PTEN on Akt1 and Akt2 reflect different properties of the pleckstrin homology (PH) domain of isoforms. Along this line, the PH domain of Akt2 may have higher affinity to $PI(3,4,5)P_3$ than $PI(3,4)P_2$, whereas the PH domain of Akt1 has similar affinities to both $PI(3,4,5)P_3$ and $PI(3,4)P_2$.

SHIP2 appears to be implicated in insulin resistance as a cause of type 2 diabetes in addition to the control of glucose homeostasis (4, 15, 16, 21, 33). SHIP2 knockout mice demonstrated enhanced phosphorylation of Akt in the skeletal muscle and liver, whereas whole body glucose homeostasis is not altered in mice fed a normal chow diet (33). However, the mice were protected from obesity and insulin resistance caused by a high-fat diet (33). Consistent with the report, the liver-specific inhibition of endogenous SHIP2 via the adenovirus-mediated expression of ΔIP-SHIP2 ameliorated glucose metabolism and insulin resistance in diabetic *db/db* mice and KK-A^y mice (8, 9). In addition, muscle denervation is known to cause insulin resistance characterized by a decrease in the ability of insulin to stimulate glucose uptake and glycogen synthesis in rats (1). A reduction of SHIP2 expression using an antisense oligonucleotide against SHIP2 mRNA ameliorated insulin resistance in rats (1). Furthermore, insulin resistance caused by chronic insulin treatment was effectively ameliorated by the expression of ΔIP-SHIP2 (29). Taken together, inhibition of endogenous SHIP2 appears to be valuable in the amelioration of insulin resistance in type 2 diabetes. Concerning the pathological impact of PTEN in glucose homeostasis (10, 13), heterozygous deletion of the PTEN gene in IRS-2 knockout mice conferred protection from insulin resistance, although homozygous disruption of the PTEN gene in mice resulted in embryonic lethality (19). Antisense oligonucleotide-mediated inhibition of endogenous PTEN expression in the liver led to the amelioration of elevated glucose levels and decreased insulin sensitivity in diabetic *ob/ob* and *db/db* mice (2). Adipose tissue-specific knockout of PTEN is known to protect against streptozotocin-induced diabetes (18). Muscle-specific knockout of PTEN resulted in the amelioration of decreased insulin-induced phosphorylation of Akt in the soleus caused by high-fat feeding (39). Although tissue-specific inhibition of PTEN may also appear to be a therapeutic target in the treatment of type 2 diabetes with insulin resistance, the main role of PTEN is the regulation of cell growth and tumor suppressor (7, 18, 34, 39); therefore, care should be taken when inhibiting PTEN for therapeutic usage because of possible tumor formation. Taken together, it is important to clarify the different molecular mechanisms by which inhibition of these lipid phosphatases ameliorates the state of insulin resistance.

TNF-α is an important adipokine causing insulin resistance by impairing insulin signaling (14, 27, 40). In the present study, we clarified that treatment with TNF-α impaired insulin-induced phosphorylation of Akt2 more profoundly than Akt1 in 3T3-L1 adipocytes. Interestingly, the expression of dominant-negative SHIP2 and PTEN enhanced the phosphorylation of Akt1 induced by insulin treatment for 120 min together with TNF-α. The present results indicate that enhancement of PI3-kinase-dependent insulin signaling by the inhibition of either lipid phosphatase is sufficient to ameliorate insulin-induced phosphorylation of Akt. Interestingly, inhibition of SHIP2, but not PTEN, effectively restored the impaired phosphorylation of Akt2 caused by TNF-α treatment. Similarly, the impaired phosphorylation of GSK3 and AS160 was ameliorated relatively more effectively by inhibition of SHIP2 than that of PTEN. Since Akt2 rather than Akt1 is closely related to the control of glucose metabolism (5), inhibition of SHIP2 rather than PTEN might be a more suitable approach to ameliorate decreased metabolic signaling of insulin in the state of insulin resistance; however, inhibition of either SHIP2 or PTEN ameliorated reduced insulin-induced glucose uptake caused by TNF-α to the same extent. It is uncertain why the extent of amelioration in glucose uptake is similar, whereas inhibition of SHIP2 improved the phosphorylation of Akt2 more than PTEN. Amelioration of Akt1 phosphorylation may be sufficient to improve glucose uptake, at least under our experimental conditions. Alternatively, the $PI(3,4,5)P_3$-mediated pathway independent of Akt may regulate glucose uptake. It might be necessary to examine the effect of glucose uptake more precisely to dissect the ameliorative role of inhibition between SHIP2 and PTEN.

In summary, the present results indicate that SHIP2 predominantly regulates insulin-induced phosphorylation of Akt2 rather than Akt1 in a time-specific manner and that PTEN regulates insulin-induced phosphorylation of both Akt1 and Akt2, whereas isoform specificity is ambiguous in the regulation in 3T3-L1 adipocytes. In addition, the expression of the dominant-negative SHIP2 effectively ameliorated decreased phosphorylation of Akt2 caused by pretreatment with TNF-α, whereas the reduced phosphorylation of Akt1 was restored by the expression of either of these phosphatase-defective lipid phosphatases without affecting the degradation of IRS-1. Our results further extend the knowledge that inhibition of both SHIP2 and PTEN is an attractive approach to ameliorate the metabolic action of insulin in the state of insulin resistance, whereas inhibition of SHIP2 appears to have more impact than PTEN on the amelioration of Akt2 phosphorylation.

ACKNOWLEDGMENTS

We thank Dr. Kazuyuki Tobe and Dr. Masashi Kobayashi for support (University of Toyama, Toyama, Japan).

GRANTS

This work was supported in part by a Grant-in-Aid for Scientific Research from the Japan Society for the Promotion of Science (to T. Sasaoka).

REFERENCES

1. **Bertelli DF, Ueno M, Amaral MEC, Toyama MH, Carneiro EM, Marangoni S, Carvalho CRO, Saad MJA, Velloso LA, Boschero AC.** Reversal of denervation-induced insulin resistance by SHIP2 protein synthesis blockade. *Am J Physiol Endocrinol Metab* 284: E679–E687, 2003.
2. **Butler M, Mckay RA, Popoff IJ, Gaarde WA, Witchell D, Murray SF, Dean NM, Bhanot S, Monia BP.** Specific inhibition of PTEN expression reverses hyperglycemia in diabetic mice. *Diabetes* 51: 1028–1034, 2002.
3. **Cantley LC.** The phosphoinositide 3-kinase pathway. *Science* 296: 1655–1657, 2002.
4. **Clement S, Krause U, Desmedt F, Tanti JF, Behrends J, Pesesse X, Sasaki T, Penninger J, Doherty M, Malaisse W, Dumont JE, Le Marchand-Brustel Y, Erneux C, Hue L, Schurmans S.** The lipid phosphatase SHIP2 controls insulin sensitivity. *Nature* 409: 92–97, 2001.
5. **Cho H, Mu J, Kim JK, Thorvaldsen JL, Chu Q, Crenshaw IIIEB, Kaestner KH, Bartolomei MS, Shulman GI, Birnbaum MJ.** Insulin resistance and a diabetes mellitus-like syndrome in mice lacking the protein kinase Akt2 (PKBβ). *Science* 292: 1728–1731, 2001.
6. **Cho H, Thorvaldsen JL, Chu Q, Feng F, Birnbaum MJ.** Akt1/PKBα is required for normal growth but dispensable for maintenance of glucose homeostasis in mice. *J Biol Chem* 276: 38349–38352, 2001.

Downloaded from ajpendo.physiology.org on February 20, 2010

7. **Di Cristofano A, Pesce B, Cordon-Cardo C, Pandolfi PP.** Pten is essential for embryonic development and tumor suppression. *Nat Genet* 19: 348–355, 1998.
8. **Fukui K, Wada T, Kagawa S, Nagira K, Ikubo M, Ishihara H, Kobayashi M, Sasaoka T.** Impact of the liver-specific expression of SHIP2 (SH2-containing inositol 5′-phosphatase 2) on insulin signaling and glucose metabolism in mice. *Diabetes* 54: 1958–1967, 2005.
9. **Grempler R, Zibrova D, Schoelch C, van Marle A, Rippmann JF, Redemann N.** Normalization of prandial blood glucose and improvement of glucose tolerance by liver-specific inhibition of SH2 domain-containing inositol phosphatase 2 (SHIP2) in diabetic KKA^{y} mice. *Diabetes* 56: 2235–2241, 2007.
10. **Hansen L, Jensen JN, Ekstrom CT, Vestergaard H, Hansen T, Pedersen O.** Studies of variability in the PTEN gene among Danish Caucasian patients with type II diabetes mellitus. *Diabetologia* 44: 237–240, 2001.
11. **Haruta T, Uno T, Kawahara J, Takano A, Egawa K, Sharma PM, Olefsky JM, Kobayashi M.** A rapamycin-sensitive pathway down-regulates insulin signaling via phosphorylation and proteasomal degradation of insulin receptor substrate-1. *Mol Endocrinol* 14: 783–794, 2000.
12. **Ishihara H, Sasaoka T, Hori H, Wada T, Hirai H, Haruta T, Langlois WJ, Kobayashi M.** Molecular cloning of rat SH2-containing inositol phosphatase 2 (SHIP2) and its role in the regulation of insulin signaling. *Biochem Biophys Res Commun* 260: 265–272, 1999.
13. **Ishihara H, Sasaoka T, Kagawa S, Murakami S, Fukui K, Kawagishi Y, Yamazaki K, Sato A, Iwata M, Urakaze M, Ishiki M, Wada T, Yaguchi S, Tsuneki H, Kimura I, Kobayashi M.** Association of the polymorphisms in the 5′-untranslated region of PTEN gene with type 2 diabetes in a Japanese population. *FEBS Lett* 554: 450–454, 2003.
14. **Iwata M, Haruta T, Usui I, Takata Y, Takano A, Uno T, Kawahara J, Ueno E, Sasaoka T, Ishibashi O, Kobayashi M.** Pioglitazone ameliorates tumor necrosis factor-α-induced insulin resistance by a mechanism independent of adipogenic activity of peroxisome proliferator-activated receptor-γ. *Diabetes* 50: 1083–1092, 2001.
15. **Kagawa S, Sasaoka T, Yaguchi S, Ishihara H, Tsuneki H, Murakami S, Fukui K, Wada T, Kobayashi S, Kimura I, Kobayashi M.** Impact of src homology 2-containing inositol 5′-phosphatase 2 gene polymorphisms detected in a Japanese population on insulin signaling. *J Clin Endocrinol Metab* 90: 2911–2919, 2005.
16. **Kaisaki PJ, Delepine M, Woon PY, Sebag-Montefiore L, Wilder SP, Menzel S, Vionnet N, Marion E, Riveline JP, Charpentier G, Schurmans S, Levy JC, Lathrop M, Farrall M, Gauguier D.** Polymorphisms in type II SH2 domain-containing inositol 5-phosphatase (INPPL1, SHIP2) are associated with physiological abnormalities of the metabolic syndrome. *Diabetes* 53: 1900–1904, 2004.
17. **Khan AH, Pessin JE.** Insulin regulation of glucose uptake: a complex interplay of intracellular signalling pathways. *Diabetologia* 45: 1475–1483, 2002.
18. **Kurlawalla-Martinez C, Stiles B, Wang Y, Devaskar SU, Kahn BB, Wu H.** Insulin hypersensitivity and resistance to streptozotocin-induced diabetes in mice lacking PTEN in adipose tissue. *Mol Cell Biol* 25: 2498–2510, 2005.
19. **Kushner JA, Simpson L, Wartschow LM, Guo S, Rankin MM, Parsons R, White MF.** Phosphatase and tensin homolog regulation of islet growth and glucose homeostasis. *J Biol Chem* 280: 39388–39393, 2005.
20. **Maehama T, Dixon JE.** The tumor suppressor, PTEN/MMAC1, dephosphorylates the lipid second messenger, phosphatidylinositol 3,4,5-triphosphate. *J Biol Chem* 273: 13375–13378, 1998.
21. **Marion E, Kaisaki PJ, Pouillon V, Gueydan C, Levy JC, Bodson A, Krzentowski G, Daubresse JC, Mockel J, Behrends J, Servais G, Szpirer C, Kruys V, Gauguier D, Schurmans S.** The gene INPPL1, encoding the lipid phosphatase SHIP2, is a candidate for type 2 diabetes in rat and man. *Diabetes* 51: 2012–2017, 2002.
22. **Nakashima N, Sharma PM, Imamura T, Bookstein R, Olefsky JM.** The tumor suppressor PTEN negatively regulates insulin signaling in 3T3-L1 adipocytes. *J Biol Chem* 275: 12889–12895, 2000.
23. **Ono H, Katagiri H, Funaki M, Anai M, Inukai K, Fukushima Y, Sakoda H, Ogihara T, Onishi Y, Fujishiro M, Kikuchi M, Oka Y, Asano T.** Regulation of phosphoinositide metabolism, Akt phosphorylation, and glucose transport by PTEN (phosphatase and tensin homolog deleted on chromosome 10) in 3T3-L1 adipocytes. *Mol Endocrinol* 15: 1411–1422, 2001.
24. **Ozes ON, Akca H, Mayo LD, Gustin JA, Maehama T, Dixon JE, Donner DB.** A phosphatidylinositol 3-kinase/Akt/mTOR pathway mediates and PTEN antagonizes tumor necrosis factor inhibition of insulin signaling through insulin receptor substrate-1. *Proc Natl Acad Sci USA* 98: 4640–4645, 1991.
25. **Pesesse X, Deleu S, De Smedt F, Drayer L, Erneux C.** Identification of a second SH2-domain-containing protein closely related to the phosphatidylinositol polyphosphate 5-phosphatase SHIP. *Biochem Biophys Res Commun* 239: 697–700, 1997.
26. **Pirola L, Johnston AM, Obberghen EV.** Modulation of insulin action. *Diabetologia* 47: 170–184, 2004.
27. **Rui L, Aguirre V, Kim JK, Shulman GI, Lee A, Corbould A, Dunaif A, White MF.** Insulin/IGF-1 and TNF-α stimulate phosphorylation of IRS-1 at inhibitory Ser307 via distinct pathways. *J Clin Invest* 107: 181–189, 2001.
28. **Saltiel AR, Kahn CR.** Insulin signalling and the regulation of glucose and lipid metabolism. *Nature* 414: 799–806, 2001.
29. **Sasaoka T, Fukui K, Wada T, Murakami S, Kawahara J, Ishihara H, Funaki M, Asano T, Kobayashi M.** Inhibition of endogenous SHIP2 ameliorates insulin resistance caused by chronic insulin treatment in 3T3-L1 adipocytes. *Diabetologia* 48: 336–344, 2005.
30. **Sasaoka T, Hori H, Wada T, Ishiki M, Haruta T, Ishihara H, Kobayashi M.** SH2-containing inositol phosphatase 2 negatively regulates insulin-induced glycogen synthesis in L6 myotubes. *Diabetologia* 44: 1258–1267, 2001.
31. **Sasaoka T, Wada T, Fukui K, Murakami S, Ishihara H, Suzuki R, Tobe K, Kadowaki T, Kobayashi M.** SH2-containing inositol phosphatase 2 predominantly regulates Akt2, and not Akt1, phosphorylation at the plasma membrane in response to insulin in 3T3-L1 adipocytes. *J Biol Chem* 279: 14835–14843, 2004.
32. **Shepherd PR, Withers DJ, Siddle K.** Phosphoinositide 3-kinase: the key switch mechanism in insulin signalling. *Biochem J* 333: 471–490, 1998.
33. **Sleeman MW, Wortley KE, Lai KMV, Gowen LC, Kintner J, Kline WO, Garcia K, Stitt TN, Yancopoulos GD, Wiegand SJ, Glass DJ.** Absence of the lipid phosphatase SHIP2 confers resistance to dietary obesity. *Nat Med* 11: 199–205, 2005.
34. **Stiles B, Wang Y, Stahl A, Bassilian S, Lee WP, Kim YJ, Sherwin R, Devaskar S, Lesche R, Magnuson MA, Wu H.** Liver-specific deletion of negative regulator Pten results in fatty liver and insulin hypersensitivity. *Proc Natl Acad Sci USA* 101: 2082–2087, 2004.
35. **Tang X, Powelka AM, Soriano NA, Czech MP, Guilherme A.** PTEN, but not SHIP2, suppresses insulin signaling through the phosphatidylinositol 3-kinase/Akt pathway in 3T3-L1 adipocytes. *J Biol Chem* 280: 22523–22529, 2005.
36. **Taniguchi CM, Emanuelli B, Kahn CR.** Critical nodes in signalling pathways: insights into insulin action. *Nat Rev Mol Cell Biol* 7: 85–96, 2006.
37. **Thong FS, Bilan PJ, Klip A.** The Rab GTPase-activating protein AS160 integrates Akt, protein kinase C, and AMP-activated protein kinase signals regulating GLUT4 traffic. *Diabetes* 56: 414–423, 2007.
38. **Wada T, Sasaoka T, Funaki M, Hori H, Murakami S, Ishiki M, Haruta T, Asano T, Ogawa W, Ishihara H, Kobayashi M.** Overexpression of SH2-containing inositol phosphatase 2 results in negative regulation of insulin-induced metabolic actions in 3T3-L1 adipocytes via its 5′-phosphatse catalytic activity. *Mol Cell Biol* 21: 1633–1646, 2001.
39. **Wijesekara N, Konrad D, Eweida M, Jefferies C, Liadis N, Giacca A, Crackower M, Suzuki A, Mak TW, Kahn CR, Klip A, Woo M.** Muscle-specific Pten deletion protects against insulin resistance and diabetes. *Mol Cell Biol* 25: 1135–1145, 2005.
40. **Yu YH, Ginsberg HN.** Adipocyte signaling and lipid homeostasis: sequelae of insulin-resistant adipose tissue. *Circ Res* 96: 1042–1052, 2005.

Downloaded from ajpendo.physiology.org on February 20, 2010

Contents lists available at ScienceDirect

Diabetes Research and Clinical Practice

journal homepage: www.elsevier.com/locate/diabres

Basic research article

Macrophage foam cell formation is augmented in serum from patients with diabetic angiopathy

Xinglong Cui[a], *Akifumi Kushiyama*[b], *Masayasu Yoneda*[a], *Yusuke Nakatsu*[a], *Ying Guo*[a], *Jun Zhang*[a], *Haruya Ono*[a], *Machi Kanna*[a], *Hideyuki Sakoda*[c], *Hiraku Ono*[d], *Takako Kikuchi*[b], *Midori Fujishiro*[c], *Masashi Shiomi*[e], *Hideaki Kamata*[a], *Hiroki Kurihara*[f], *Masatoshi Kikuchi*[b], *Shoji Kawazu*[b], *Fusanori Nishimura*[g], *Tomoichiro Asano*[a,*]

[a] *Department of Medical Chemistry, Division of Molecular Medical Science, Graduate School of Biomedical Science, Hiroshima University, 1-2-3 Kasumi, Minami-ku, Hiroshima City, Hiroshima, Japan*

[b] *The Institute for Adult Diseases, Asahi Life Foundation, 1-6-1 Marunouchi, Chiyoda-ku, Tokyo, Japan*

[c] *Department of Internal Medicine, Graduate School of Medicine, University of Tokyo, 7-3-1 Hongo, Bunkyo-ku, Tokyo, Japan*

[d] *Department of Medicine, Diabetes Research Center, Albert Einstein College of Medicine, New York, NY, USA*

[e] *Institute for Experimental Animals, Kobe University School of Medicine, Kobe, Hyogo, Japan*

[f] *Physiological Chemistry and Metabolism, Graduate School of Medicine, University of Tokyo, Bunkyo-ku, Tokyo, Japan*

[g] *Department of Dental Science for Health Promotion, Division of Cervico-Gnathostomatology, Graduate School of Biomedical Sciences, Hiroshima University, Japan*

ARTICLE INFO

Article history:
Received 3 April 2009
Received in revised form
18 October 2009
Accepted 22 October 2009
Published on line 24 November 2009

Keywords:
Macrophage
Diabetic angiopathy
Ex vivo assay
Foam cell

ABSTRACT

The differentiation of macrophages into cytokine-secreting foam cells plays a critical role in the development of diabetic angiopathy. J774.1, a murine macrophage cell line, reportedly differentiates into foam cells when incubated with oxidized LDL, ApoE-rich VLDL or WHHLMI (myocardial infarction-prone Watanabe heritable hyperlipidemic) rabbit serum. In this study, serum samples from Type 2 diabetic patients were added to the medium with J774.1 cells and the degree of foam cell induction was quantified by measuring lipid accumulation. These values were calculated relative to the activities of normal and WHHLMI rabbit sera as 0% and 100%, respectively, and termed the MMI (Macrophage Maturation Index). These MMI values reflected intracellular lipids, including cholesteryl ester assayed by GC/MS. Statistical analysis revealed MMI to correlate positively and independently with serum triglycerides, the state of diabetic retinopathy, nephropathy and obesity, but negatively with administration of α-glucosidase inhibitors or thiazolidinediones. Taken together, our results suggest that this novel assay may be applicable to the identification of patients at risk for rapidly progressive angiopathic disorders.

© 2009 Elsevier Ireland Ltd. All rights reserved.

* *Corresponding author.* Tel.: +81 332016781; fax: +81 332016881.
E-mail address: asano-tky@umin.ac.jp (T. Asano).

Abbreviations: BS, blood sugar; sBP, systolic blood pressure; dBP, diastolic blood pressure; TC, total cholesterol; TG, triglyceride; SU, sulfonylurea; α-GI, α-glucosidase inhibitor; BG, Biguanide; TZD, thiazolidinedione; eGFR, estimated glomerular filtration ratio; GC, gas chromatography; AUC, area under the curve.

0168-8227/$ – see front matter © 2009 Elsevier Ireland Ltd. All rights reserved.
doi:10.1016/j.diabres.2009.10.011

1. Introduction

Macrophages play important roles in the progression of both diabetic microangiopathy [1,2] and macroangiopathy [3–5]. Macrophages invade the dysfunctional vascular endothelium, change into foam cells by taking up lipids, and secrete high levels of several inflammatory hormones, as well as matrix metalloproteases, which contribute to the development of pathological lesions and remodeling. Indeed, foam cells appear even in the early stages of angiopathy, and the accumulation of large numbers of foam cells is often observed in advanced lesions.

Considering that numbers of patients with diabetic angiopathy and metabolic syndrome are rising dramatically worldwide, it is important to develop a method of identifying those with rapidly progressive angiopathic lesions. In this study, we measured patient serum activity inducing the differentiation of J774.1 into foam cells. During foam cell formation from macrophages, numerous factors including oxidized LDL play an enhancing role [6,7], but J774.1 cells reportedly differentiate into foam cells when incubated with oxidized low density lipoprotein (LDL), very low density lipoprotein (VLDL), or myocardial infarction-prone Watanabe heritable hyperlipidemic (WHHLMI) rabbit serum [8]. The WHHLMI rabbit was developed from WHHL rabbits [9], which have a mutated LDL receptor and hypercholesterolemia, such that atherosclerosis develops rapidly [10,11]. The incidence of myocardial infarction in WHHL rabbits was low, while WHHLMI rabbits developed coronary occlusion and spontaneous myocardial infarction reportedly due to having higher amounts of apolipoprotein E-rich VLDL [12–14].

We investigated whether serum activities in diabetic patients inducing the differentiation of J774.1 cells into foam cells, differ according to patient features including metabolic control, development of angiopathic complications, drug treatments, and so on. Our statistical analysis revealed that foam cell-inducing activity correlates positively and independently with serum triglycerides (TG), the state of diabetic retinopathy, nephropathy and obesity, but negatively with administration of α-glucosidase inhibitors (α-GI) or thiazolidinediones (TZD). Such an assay was thus suggested to possibly be applicable to identifying patients at risk for rapidly progressing angiopathic disorders.

2. Materials and methods

2.1. *Reagents and cell culture*

Murine macrophage-like J774.1 cells were purchased from Riken (Tsukuba, Japan), cultured in RPMI 1640 (Sigma) medium supplemented with 10% fetal calf serum (FCS) (Invitrogen), Penicillin 100 U/ml and Streptomycin 100 μg/ml (GIBCO Invitrogen) at 37 °C in 5% CO_2. All reagents were of analytical grade.

Cells were cultured on 96 well plates (IWAKI) for serum stimulation and lipid accumulation assays. At 90% confluence, each well was incubated with serum free RPMI1640 for 24 h, and then stimulated with 2% serum from individual patients for 72 h. The cells were then subjected to lipid accumulation

Table 1 – (a) Coefficients of correlation and their significance for parametric variables and MMI. (b) Means of MMI for all groups classified by non-parametric complications and use of medications. Values are given as means ± SE. (c) Partial regression coefficients and their significances, for variables adjusted for each other but not normalized. Significance is represented by the *p* values at the bottom.

	Coefficients	*p* value
a.		
Age	−0.025	0.827
BS	0.249	0.030*
HbAlc	0.254	0.027*
sBP	0.068	0.562
dBP	0.075	0.518
WBC	0.246	0.032*
AST	0.012	0.917
ALT	0.134	0.248
γGTP	0.146	0.208
TC	−0.077	0.507
HDL	−0.509	2.55×10^{-6}***
TG	0.528	9.68×10^{-7}***
BMI	0.257	0.025*
Cre	0.259	0.024*
eGFR	−0.188	0.104
	−	+
b.		
Gender (M/F)	19.27 ± 4.97	13.33 ± 1.24
Retinopathy	13.18 ± 1.38	26.07 ± 7.54**
Proteinuria	12.05 ± 1.14	25.46 ± 5.91*
IHD	15.35 ± 1.82	11.55 ± 3.09
SU	14.47 ± 2.57	15.69 ± 2.18
α-GI	15.83 ± 2.03	12.12 ± 2.61
TZD	14.80 ± 1.82	17.88 ± 3.10
BG	12.03 ± 1.25	20.85 ± 4.14*
Insulin	13.10 ± 1.57	18.79 ± 3.87
Anti-RA	11.09 ± 1.11	20.54 ± 3.52*
Statin	13.13 ± 1.27	18.73 ± 4.27
Anti-platelet	14.43 ± 0.96	22.22 ± 15.36
	Coefficients	*p* value
c.		
(Intercept)	19.55	0.544
Age	−0.282	0.029*
BS	0.005	0.869
HbAlc	−1.211	0.388
sBP	0.072	0.286
dBP	−0.129	0.231
WBC	0.043	0.560
AST	0.324	0.140
ALT	−0.196	0.179
γGTP	0.005	0.938
TC	−0.086	0.022*
HDL	0.046	0.593
TG	0.088	3.66×10^{-8}***
BMI	0.590	0.099†
Cre	0.496	0.952
eGFR	0.002	0.986
Gender	0.307	0.926
Retinopathy	9.304	0.029*
Proteinuria	9.363	0.017*
IHD	−7.429	0.152
CVD	3.128	0.728
SU	−1.551	0.541
α-GI	−6.307	0.018*

Table 1 (*Continued*)

	Coefficients	*p* value
TZD	−8.273	0.158
BG	4.333	0.088†
Insulin	−1.578	0.637
Anti-RA	−0.641	0.802
Statin	0.789	0.748
Anti-platelet	−4.185	0.312

* $p < 0.05$.
** $p < 0.01$.
*** $p < 0.001$.
† $p < 0.1$.

assays using AdipoRed (Cambrex), according to the manufacturer's instructions [15]. In brief, the cells were carefully rinsed with phosphate buffered saline (PBS), and 5 μl of AdipoRed reagent were then added to 200 μl of PBS, followed incubation for 10 min at room temperature. Fluorescence was measured with excitation and emission wavelengths of 485 nm and 572 nm, respectively, by fluorimetry. The value obtained with 2% WHHLMI rabbit serum incubation was taken as the Macrophage Maturation Index (MMI) of 100, while 2% normal rabbit serum incubation yielded an MMI of zero. A calibration curve was obtained by serial dilutions of WHHLMI with normal serum. One raw value was the mean, in relative fluorescence units, of five areas per well, and assays were performed five times to obtain a mean MMI value.

2.2. *Serum sampling*

The subjects were 76 patients (53 males and 23 females), who underwent serum sampling in hospitals affiliated with the Institute for Adult Disease, Asahi Life Foundation. The blood examination data and clinical presentations of patients, obtained in routine clinical practice, were collected at the same time as serum sampling. Stage of diabetic retinopathy was determined within 12 months prior to blood sampling, and stage at the last fundus examination was adopted if several examinations had been performed due to stage instability during the prior 12-month period. Patient characteristics are presented in Table 1. All subjects gave informed consent and the study was verified by the institutional ethics committee.

2.3. *Lipid extraction, purification, and separation by GC/MS*

To analyze lipid profiles of accumulated intracellular lipids in J774.1 cells, total lipids were extracted and purified by the Folch method, as previously described [16]. Then, the lipids were dissolved in *n*-hexane and 1 μl of sample was injected into an RTX-5MS (0.25 mm ID × 30 m, 0.25 μm) column attached to a gas chromatograph (Thermo Finnigan Trace GC 2000) which was connected to a mass spectrometer (Thermo Finnigan Trace MS: scanning range: 1–600 *m/z*). The injection temperature was 250 °C, and oven temperatures were 100 °C (2 min) → (25 °C/min) → 250 °C (20 min) → (10 °C/min) → 270 °C (10 min). Cholesteryl components were detected at 362–368 *m/z* independently of other substances.

2.4. *Statistical analysis*

We quantified non-parametrical data such as type of medication, and the state of diabetic complications into indicator variables. Diabetic neuropathy was not assessed because of its variable clinical presentations, which cannot be quantified adequately for transformation into a simple dummy variable and thus could not be effectively utilized in the relatively small number of subjects in this study. Diabetic retinopathy was initially recorded using the Fukuda Classification [17], and stage A2 or later on the most severely affected side, i.e. active and progressive states of retinopathy, were dummied as 1, others as 0. Stage of diabetic nephropathy was omitted because diagnosing nephropathy by estimated glomerular filtration ratio (eGFR) and proteinuria was deemed redundant. The presence of ischemic heart disease (IHD) and/or cardiovascular disease (CVD) was determined based on past events, or past and ongoing therapies for these disorders. All ongoing medical therapy classified in Table 1 was dummied as 1 and others 0, dosage-independently.

Data organizing was achieved with Excel2000 (Microsoft), and hierarchical cluster analysis, described using GENESIS 1.7.2 (IGB-TUG). Other statistical analyses were performed using R 2.6.2 (The R Foundation for Statistical Computing), i.e. one-way ANOVA, principal component analysis, multi-regression analysis and logistic regression analysis. The Akaike information criterion (AIC) was used to select the best of a collection of candidate models for this dataset.

3. Results

3.1. *Macrophage Maturation Index*

In the macrophage cell line J774.1, administering WHHLMI rabbit serum (final conc. 2%) time-dependently increased macrophage foaming, and lipid accumulation was observed (Fig. 1a) and quantified (Fig. 1b). WHHLMI rabbits exhibit hypercholesterolemia and hypertriglyceridemia, and develop atherosclerosis spontaneously *in vivo* [9]. Their serum thus has the capacity to induce macrophage foaming *ex vivo*. We termed the relative value of lipid accumulation at 72 h, standardized by serial dilution of serum from a WHHLMI rabbit, the MMI. The intra-assay coefficient of variation (CV) was 5.60% ($n = 8$) and the inter-assay CV was 9.43% ($n = 6$). This bioassay was affected by the status of the J774.1 cell line. Thus, assays must be performed with careful attention to cell viability.

We next investigated the MMI of Type 2 diabetic patients whose characteristics are presented in Table 1, and obtained a value of 15.02 ± 14.76 (Supple. 1).

3.2. *Mining the MMI and other datasets*

To clarify the relationships between MMI and other variables, we obtained sera from patients undergoing routine medical investigations. We organized and applied the data to the following analysis. As shown in Fig. 2a, data from all patients were normalized by variables and aligned in ascending order of MMI values. Herein, a tendency for clinical presentation

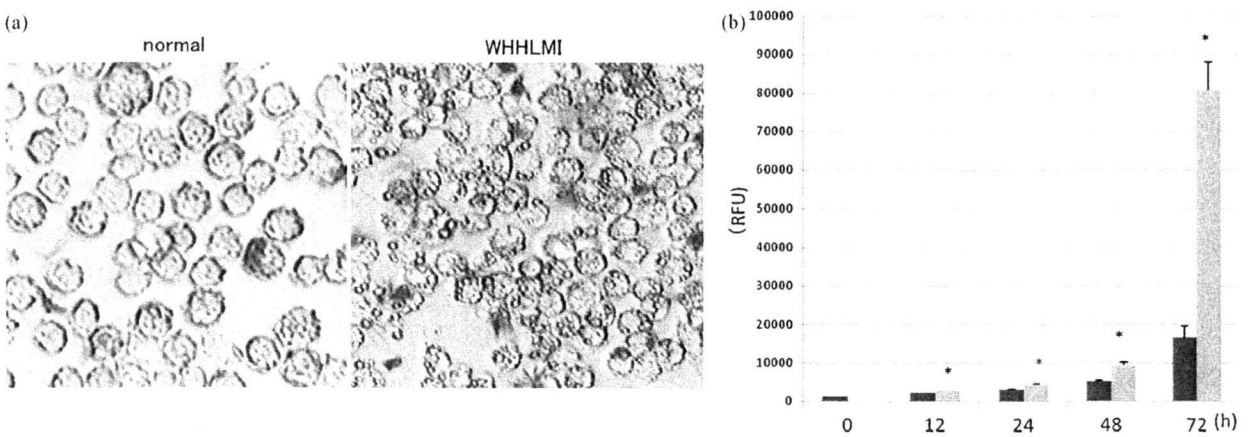

Fig. 1 – (a) Murine macrophage-like cell foaming and lipid accumulation. Cells were cultured on 96-well plates for serum stimulation and lipid accumulation assays. At 90% confluence, each well was incubated with serum free medium for 24 h, and then stimulated with 2% serum from normal and WHHLMI rabbits for 72 h. The cells were then subjected to lipid accumulation assays using Oil red O staining for presentation as an optical microscope image, and using AdipoRed (Cambrex) for quantification. (b) Quantification of lipid accumulation in a time-dependent manner. The cells were carefully rinsed with PBS, and 5 μl of AdipoRed reagent were then added to 200 μl of PBS, followed by incubation for 10 min at room temperature. Fluorescence was measured with excitation and emission wavelengths of 485 nm and 572 nm, respectively, by fluorimetry. One raw value served as the mean of the relative fluorescence, in units, of five areas. The assays were performed five times to obtain a mean MMI value.

with a high MMI to correlate with high Cre, HbA1c, proteinuria and diabetic retinopathy was already apparent, while a low MMI reflected α-GI administration. In Fig. 2b, hierarchical clustering of variables is shown. MMI clustered with TG and renal function. Other variables showed clustering with each other. Only two subjects had CVD, such that power was inadequate for significant variables to be identified by any test. Thus, subjects with CVD were included among those with IHD.

MMI and originally parametric variables are presented in Table 1a. Significant correlations existed between MMI and variables concerning blood glucose control (BS, HbA1c), the inflammatory state (WBC), lipid profile (HDL, TG) and renal function (Cre). When MMI was classified by groups of complications or medications administered, formed retinopathy, proteinuria and administration of BG and anti-RA were associated with significantly higher MMI. Only α-GI administration tended to be associated with lower MMI. With MMI as a criterion variable and others as predictor variables, partial coefficients for regression were calculated, as shown in Table 1c. There was an independent relation between MMI and each variable. Some variables showed inverse correlations or differing significance for the datasets in Table 1a and c, and

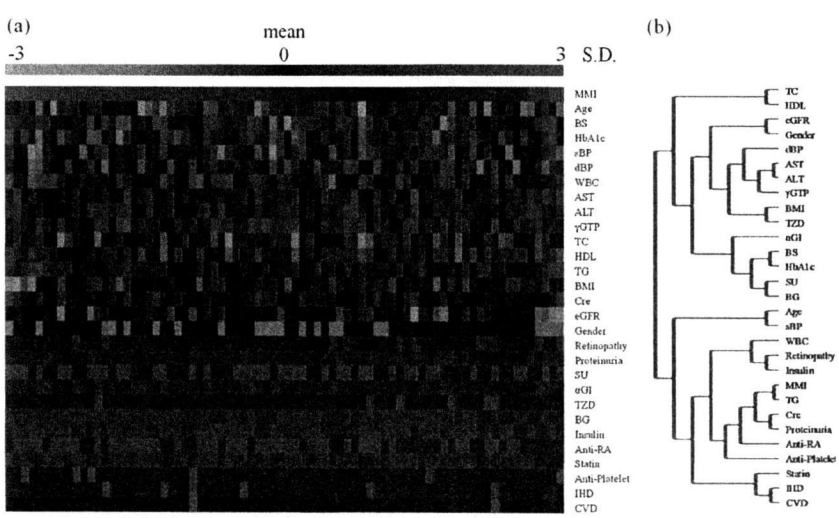

Fig. 2 – (a) Optical presentation of all normalized data from subjects. Parameters were normalized by variables and visualized using GENESIS 1.7.2. Data were aligned in ascending order by MMI from the left for every subject. The tendency was already qualitatively apparent. (b) Hierarchical clustering analysis of variables. Variables presented similar patterns, being clustered in one neighborhood.

Table 2 – Model for multiple regression analysis. Variables were selected by AIC from the variables in Fig. 2. Model: MMI = a × TG (mg/dl) + b × BMI (kg/m^2) + c × (retinopathy) + d × (proteinuria) + e × (α-GI) + f × (TZD) + g.

	Coefficients		Estimated SE	p value
(Intercept)	g	−16.97	5.86	0.0051**
TG	a	0.079	0.0076	8.6×10^{-16}***
BMI	b	0.77	0.24	0.0022**
Retinopathy	c	8.79	2.72	0.0019**
Proteinuria	d	8.28	2.23	0.0004***
α-GI	e	−7.54	2.24	0.0012**
TZD	f	−10.57	3.80	0.0069**

Multiple R^2: 0.75. Adjusted R^2: 0.72.
** $p < 0.01$.
*** $p < 0.001$.

between those in Table 1b and c, probably due to the clinically well-known multi-colinearity (*e.g.* AST and ALT, HDL and TG). In principal component analysis (data not shown), MMI, BS, HbA1c, WBC, HDL, TG, BMI, Cre, retinopathy, proteinuria, BG, Ins, Anti-RA, statin and Anti-Platelet medications were the first principal components.

3.3. *Modeling to account for MMI from routinely obtained parameters*

We subsequently attempted to model a linearly combined collection of variables using stepwise multi-regression analysis. In the model in Table 2, 72% of the variability of MMI was accounted for by variables specified in the model from the adjusted *R*-squared value. Selection of variables was performed using AIC, that is, the relations of MMI to the variables examined in these models were assumed to be stronger than those of residual variables. Values of TG and BMI, the existence of active retinopathy and/or proteinuria, and administrations of α-GI and TZD were determined and their significance was assessed. Coefficients were not standardized in the model, and thus showed gradients for variables reflecting their own measurement units. For instance, a 1 mg/dl rise in TG proportionally indicated an increase of 0.079, diabetic retinopathy an increase of 8.79, and α-GI administration a reduction of 7.54 in MMI. The fitness of the model is described in Supple. 2 as a QQ plot, basically showing a well-fitted and seemingly appropriate model.

TG was the strongest, possibly even excessively influential, variable. However, if our subjects were limited to those with TG values of no more than 300 mg/dl, the TG effect was no longer selected, and BS, AST, HDL and anti-platelet therapy were newly included in the model. BG administration had a reciprocally worsening effect but it was not significant, and diabetic angiopathies and α-GI were still selected, much as in the model shown in Supple. 3. If the strongest TG effect dissipated, 46.51% was still accounted for by the parameters of the adjusted R^2 value despite the smaller subject number.

3.4. *Prediction of diabetic angiopathy activity by MMI*

Sera from patients with both retinopathy and proteinuria exhibited higher MMI than those from patients with either retinopathy or proteinuria (Fig. 3a). To investigate qualitatively whether MMI predicts diabetic angiopathy, a logistic regression analysis was performed (Fig. 3b), using diabetic angiopathy as the criterion variable, and the risk ratio was then estimated. When MMI rose to +1SD (14.76), the risk ratio (RR) for retinopathy was 1.36 (1.10–1.69, 95% C.I.) and the RR adjusted by all other variables was 1.55 (1.06–2.26). The RR for proteinuria was 1.46 (1.18–1.80), the adjusted RR 1.54 (1.10–2.18).

3.5. *Relationships between cholesteryl ester accumulation and MMI*

Relationships of the MMI values and extracted lipid profiles using GC/MS are presented in Supple. 4a and b. In Supple. 4a, a representative GC chart is shown, and the cholesteryl components detected are shown in Supple. 4b. The sum of the AUCs of cholesteryl ester, other lipids (including FFAs, glycerides analyzed from MS data), and total AUCs tended to correlate positively with MMI (Supple. 5).

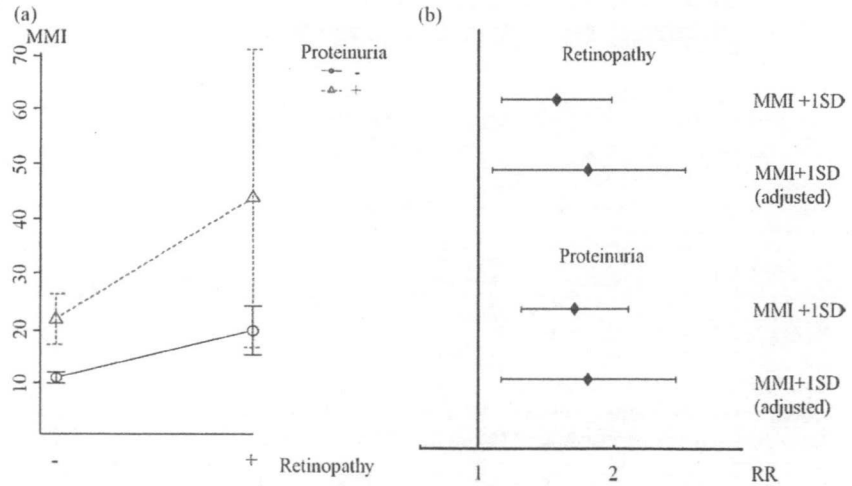

Fig. 3 – (a) Relationships of diabetic angiopathy variables and MMI. Retinopathy and proteinuria together were associated with higher MMI than either retinopathy or proteinuria alone. (b) Risk ratio against increment of MMI (+1SD, 14.76) estimated using logistic regression analysis.

4. Discussion

It is well known that both macroangiopathy and microangiopathy tend to develop rapidly in patients with poorly controlled diabetes. Numerous factors present in macroangiopathy and microangiopathy such as hypertension [18,19], hyperglycemia [20], hyperinsulinemia [21,22], hyperlipidemia [7,23], oxidative stress [24,25] and so on, contribute to angiopathic progression via independent and/or coordinated mechanisms [6,21,24]. Some of these numerous effects act directly on vascular cells [26], while others affect macrophages which invade vascular cells [6]. In this study, we focused on foam cell formation from macrophages, and the activities of patient sera which induce foam cell differentiation were measured. The sera were obtained from diabetic patients, because atherosclerosis and microangiopathy develop rapidly in this patient population. To obtain reproducible values, we used the J774.1 cell line which firmly attaches to culture-dishes and changes into foam cells in response to WHHLMI rabbit serum. Assay reproducibility and validity were confirmed from intra-assay and inter-assay CVs. However, as CVs were still somewhat high, cautious cell handling is critical before proceeding to clinical use. Moreover, by GC analysis, lipid accumulation including cholesteryl ester accumulation rose in proportion to the MMI increase. No specific GC peak corresponding to MMI was detectable. Therefore, the AdipoRed assay precisely reflects intracellular lipid ester accumulation. The obtained values were thus used for comparisons with various clinical factors.

MMI was revealed to be clustered with TG and diabetic nephropathy, the latter being a well-known cause of hypertriglyceridemia [27]. Furthermore, diabetic retinopathy was relatively closely related to MMI and was presumed to be an event preceding nephropathy. Among partial coefficients of regression, age was negative and significant, in fact dovetailing with newly progressive retinopathy being less severe in elderly patients [28].

In multiple regression analysis, we selected six variables which rather strongly accounted for MMI. TG itself is thought to be the primary material of intra-TG accumulation. TZDs might have direct effects against macrophages, while with diabetic retinopathy and nephropathy, administration of an α-GI, which is minimally absorbed from the intestinal tract, and a high BMI reflect only the clinical state and are not directly related to serum parameters. Among these, α-GIs improve blood sugar fluctuations, and a high BMI (obesity) is known to produce metabolic syndrome, the major cause of insulin resistance and atherosclerotic angiopathy. From this viewpoint, it is reasonable that TZDs suppress the ill effects of obesity, by improving insulin resistance. To develop a practical assay, the system shown in the Supple. 3 Table might be worthwhile. It might actually be the case that numerous pathways and bioactive substances affect macrophage maturation in the absence of any lipid effect. Logistic regression analysis, conversely, revealed MMI to be useful for measuring the activity or progression of diabetic angiopathy. In other words, macrophage foam cell formation was related to the development of diabetic microangiopathy. At a minimum, active retinopathy and nephropathy at stage 3a or later were predictable from a higher MMI value at the same time point. Retinopathy and nephropathy acted simply in an additive manner with MMI, suggesting that a higher number of complications reflect the strength of macrophage activity.

Several clinical studies have focused on diabetic angiopathy and medications, with subsets of drugs proving to be effective against angiopathy, though the underlying mechanisms remain uncertain. The α-GIs and TZDs were demonstrated to be effective for the prevention of macrovascular diseases in the stop-NIDDM trial [29] and the PROactive study [30], respectively. However, whether or not this is attributable to direct and/or indirect effects on atherosclerotic regions rather than glycemic control remains unclear. Taking the results of this assay into consideration, these medications may function to prevent macrophage foaming. Moreover, we found that MMI reflected several factors, including foaming or lipid accumulation in individual cells, as well as cell viability and/or growth. Intensive studies focusing on both the characteristics of serum, *i.e.* analysis by 2-DE/mass spectrometry, and the corresponding effects on macrophages, *i.e.* microarray investigations, might clarify the features of macrophage activation.

This study was cross-sectional, such that relationships among variables were ambiguous in terms of cause and effect, especially the impacts of medical therapy. Most of the diabetic patients examined had already received interventional therapies including not only anti-hyperglycemic agents, but also anti-hypertensive agents, statins, anti-coagulants, and so on. Although a future intensive cohort study is needed, MMI might be corrected to avoid excessively strong effects of the lipid state, thus truly reflecting the risk of developing angiopathic diseases in patients with Type 2 diabetes, and thereby become a useful indicator for selecting appropriate medical therapy.

Acknowledgements

We are deeply grateful to Hirokazu Sato and Yuko Oki for their technical supports. This work was supported by a Grant-in-Aid for Exploratory Research from the Japan Promotion of Science Foundation of the Japanese Government.

Appendix A. Supplementary data

Supplementary data associated with this article can be found, in the online version, at doi:10.1016/j.diabres.2009.10.011.

Conflict of interest

There are no conflicts of interest.

REFERENCES

[1] Tesch, Role of macrophages in complications of type 2 diabetes, Clin. Exp. Pharmacol. Physiol. 34 (2007) 1016–1019.
[2] Nguyen, Ping, Mu, Hill, Atkins, Chadban, Macrophage accumulation in human progressive diabetic nephropathy, Nephrology (Carlton) 11 (2006) 226–231.

Author's personal copy

[3] Boyle, Diabetes mellitus and macrovascular disease: mechanisms and mediators, Am. J. Med. 120 (2007) S12–17.
[4] Simionescu, Implications of early structural-functional changes in the endothelium for vascular disease, Arterioscler. Thromb. Vasc. Biol. 27 (2007) 266–274.
[5] Gacka, Dobosz, Szymaniec, Bednarska-Chabowska, Adamiec, Sadakierska-Chudy, Proinflammatory and atherogenic activity of monocytes in Type 2 diabetes, J. Diabetes Complications (2008).
[6] Hodgkinson, Laxton, Patel, Ye, Advanced glycation end-product of low density lipoprotein activates the toll-like 4 receptor pathway implications for diabetic atherosclerosis, Arterioscler. Thromb. Vasc. Biol. 28 (2008) 2275–2281.
[7] Ishigaki, Katagiri, Gao, Yamada, Imai, Uno, et al., Impact of plasma oxidized low-density lipoprotein removal on atherosclerosis, Circulation 118 (2008) 75–83.
[8] Mori, Itabe, Higashi, Fujimoto, Shiomi, Yoshizumi, et al., Foam cell formation containing lipid droplets enriched with free cholesterol by hyperlipidemic serum, J. Lipid Res. 42 (2001) 1771–1781.
[9] Shiomi, Ito, Yamada, Kawashima, Fan, Development of an animal model for spontaneous myocardial infarction (WHHLMI rabbit), Arterioscler. Thromb. Vasc. Biol. 23 (2003) 1239–1244.
[10] Tanzawa, Shimada, Kuroda, Tsujita, Arai, Watanabe, WHHL-rabbit: a low density lipoprotein receptor-deficient animal model for familial hypercholesterolemia, FEBS Lett. 118 (1980) 81–84.
[11] Buja, Kita, Goldstein, Watanabe, Brown, Cellular pathology of progressive atherosclerosis in the WHHL rabbit. An animal model of familial hypercholesterolemia, Arteriosclerosis 3 (1983) 87–101.
[12] Shiomi, Ito, Shiraishi, Watanabe, Inheritability of atherosclerosis and the role of lipoproteins as risk factors in the development of atherosclerosis in WHHL rabbits: risk factors related to coronary atherosclerosis are different from those related to aortic atherosclerosis, Atherosclerosis 96 (1992) 43–52.
[13] Ishii, Kita, Yokode, Kume, Nagano, Otani, et al., Characterization of very low density lipoprotein from Watanabe heritable hyperlipidemic rabbits, J. Lipid Res. 30 (1989) 1–7.
[14] Ito, Yamada, Shiomi, Progression of coronary atherosclerosis relates to the onset of myocardial infarction in an animal model of spontaneous myocardial infarction (WHHLMI rabbits), Exp. Anim. 53 (2004) 339–346.
[15] Greenspan, Fowler, Spectrofluorometric studies of the lipid probe, nile red, J. Lipid Res. 26 (1985) 781–789.
[16] Kushiyama, Shojima, Ogihara, Inukai, Sakoda, Fujishiro, et al., Resistin-like molecule beta activates MAPKs, suppresses insulin signaling in hepatocytes, and induces diabetes, hyperlipidemia, and fatty liver in transgenic mice on a high fat diet, J. Biol. Chem. 280 (2005) 42016–42025.
[17] Fukuda, Classification and treatment of diabetic retinopathy, Diabetes Res. Clin. Pract. 24 Suppl. (1994) S171–176.
[18] Veglio, Paglieri, Rabbia, Bisbocci, Bergui, Cerrato, Hypertension and cerebrovascular damage, Atherosclerosis (2008).
[19] Silva, Pinto, Biswas, de Faria, de Faria, Hypertension increases retinal inflammation in experimental diabetes: a possible mechanism for aggravation of diabetic retinopathy by hypertension, Curr. Eye Res. 32 (2007) 533–541.
[20] Avogaro, de Kreutzenberg, Fadini, Endothelial dysfunction: causes and consequences in patients with diabetes mellitus, Diabetes Res. Clin. Pract. 82 Suppl. 2 (2008) S94–S101.
[21] Vaidyula, Boden, Rao, Platelet and monocyte activation by hyperglycemia and hyperinsulinemia in healthy subjects, Platelets 17 (2006) 577–585.
[22] Sugimoto, Baba, Suda, Yasujima, Yagihashi, Peripheral neuropathy and microangiopathy in rats with insulinoma: association with chronic hyperinsulinemia, Diabetes Metab. Res. Rev. 19 (2003) 392–400.
[23] Yang, Shi, Hao, Li, Le, Increasing oxidative stress with progressive hyperlipidemia in human: relation between malondialdehyde and atherogenic index, J. Clin. Biochem. Nutr. 43 (2008) 154–158.
[24] Ogihara, Asano, Katagiri, Sakoda, Anai, Shojima, et al., Oxidative stress induces insulin resistance by activating the nuclear factor-kappa B pathway and disrupting normal subcellular distribution of phosphatidylinositol 3-kinase, Diabetologia 47 (2004) 794–805.
[25] Osto, Matter, Kouroedov, Malinski, Bachschmid, Camici, et al., c-Jun N-terminal kinase 2 deficiency protects against hypercholesterolemia-induced endothelial dysfunction and oxidative stress, Circulation 118 (2008) 2073–2080.
[26] Kakehashi, Inoda, Mameuda, Kuroki, Jono, Nagai, et al., Relationship among VEGF, VEGF receptor, AGEs, and macrophages in proliferative diabetic retinopathy, Diabetes Res. Clin. Pract. 79 (2008) 438–445.
[27] Yoshino, Hirano, Nagata, Maeda, Naka, Murata, et al., Hypertriglyceridemia in nephrotic rats is due to a clearance defect of plasma triglyceride: overproduction of triglyceride-rich lipoprotein is not an obligatory factor, J. Lipid Res. 34 (1993) 875–884.
[28] Wong, Molyneaux, Constantino, Twigg, Yue, Timing is everything: age of onset influences long-term retinopathy risk in type 2 diabetes, independent of traditional risk factors, Diabetes Care 31 (2008) 1985–1990.
[29] Chiasson, Josse, Gomis, Hanefeld, Karasik, Laakso, Acarbose for prevention of type 2 diabetes mellitus: the STOP-NIDDM randomised trial, Lancet 359 (2002) 2072–2077.
[30] PROactive study, Lancet 367 (2006) 982.